NATIONAL CENTER FOR ATMOSPHERIC RESEARCH
BOULDER, COLORADO

20 December 1965
Recd 24/12/65

Mr. Grote Reber
CSIRO
Stowell Avenue
Hobart, Tasmania

Posted 20/12/65 7oz.
Recd 27/12/65 air mail
$3,50 postage

Dear Mr. Reber:

Thank you very much for your paper on the atmospheric pressure oscillations at Haleakala. I am sending you under separate cover my paper on the diurnal pressure oscillation presented at the NAS meeting (Reprint from Archiv) and three additional papers which may be of interest to you.

For further references on the whole subject I recommend an article by S. Chapman in The Compendium of Meteorology and an article by M. Siebert in Advances in Geophysics, vol. 7 (1961), pp. 105-187. The largest collection of data on S_3, the 8-hourly oscillation, is contained in a paper by Hann in Denkschriften der Kaiserlichen Akademie der Wissenschaften in Wien, Math.-Nat. Kl., vol. 95 (1917), pp. 1-64. There have, of course, been additional determinations of S_3 since that time. For instance, in the paper by Mrs. Cowley and myself, which is being mailed to you, this oscillation is determined incidentally as part of an investigation of the lunar air tide.

Sincerely yours,

B. Haurwitz

Bernhard Haurwitz

THE LUNAR AND SOLAR AIR TIDES AT SIX STATIONS IN NORTH AND CENTRAL AMERICA

B. HAURWITZ AND ANN D. COWLEY

National Center for Atmospheric Research, Boulder, Colo.

ABSTRACT

The lunar semidiurnal tide and the solar 24-, 12-, 8-, and 6-hour oscillations have been determined for the six stations Balboa, Panama; San Juan, P.R.; Aguadilla, P.R.; Burbank, Calif.; Oklahoma City, Okla.; and Greensboro, N.C.

1. INTRODUCTION

The lunar atmospheric tide is of great theoretical interest because it shows the response of the atmosphere to a completely known external force, namely the tidal attraction of the moon. This interest has been further increased in recent years since it appears that a lunar period may be present not only in such meteorological parameters as pressure, wind, and temperature, but also in precipitation (for instance, [4]), and sunshine duration [10].

The best documented manifestation of the lunar air tide is the semidiurnal (lunar) surface pressure oscillation. Largely through the efforts of S. Chapman and numerous collaborators (for instance, [6]) this period is now known for more than 70 stations. These stations show that the distribution of the lunar tide is not entirely regular over the earth despite the regularity of the moon's tidal force. For about 60 of these stations the variation of the lunar tide with the seasons, which is in the same sense in both hemispheres, has also been determined: In general, the amplitude maximum occurs during the northern summer, and the daily high tides are reached latest during the northern winter.

In order to increase our knowledge of the global distribution of the lunar tide, a study has been started to analyze further data, and the present paper reports in part the results of this analysis for the first six stations. These stations with the relevant information are shown in table 1. Only the pressure oscillations will be discussed here. Results of analyses of wind and temperature (not successful in the case of the lunar tide) will be reported later.

The observational data used for the tidal determinations were made available by the National Weather Records Center in Asheville, N.C. Bi-hourly values of the pressure were used, with the first hour being 0 (midnight) Local Standard Time. The whole material was subdivided into the three "seasons" commonly used in air-tidal studies, namely

D: November, December, January, February
J: May, June, July, August
E: March, April, September, October (Equinoctial months)

In each of these seasons the days were further grouped according to the daily lunar phase integer L (in its modified form which moves from 0 to 11 twice during the synodic month). For the years 1961 and 1962 these integers were computed by means of tables given by Bartels and Fanselau [3]. For the earlier years punched cards based on a compilation by Bartels [2] were made available by Dr. J. C. Cain of the Goddard Space Flight Center at NASA.

For the stations Balboa, Oklahoma City, Greensboro, and Burbank the required bi-hourly mean values of the surface pressures for the different groups were computed by the National Weather Records Center. The harmonic analysis of these values was performed on an IBM 1620 computer at the High Altitude Observatory of NCAR.

TABLE 1.—*List of stations*

Station	Lat. (°N.)	Long. (°W.)	Alt. (ft.)	Years of Record	Number of Days
Balboa, Panama	9.0	79.5	20	Mar. 1941—June 1958	6156
San Juan, P.R.	18.5	66.1	60-80	Mar. 1945—April 1962	6142
Aguadilla, P.R. (Ramey AFB)	18.5	67.1	220	Jan. 1941—June 1958	6217
Burbank, Calif.	34.2	118.4	725	Jan. 1942—April 1945 Jan. 1948—Dec. 1962	6589
Oklahoma City, Okla.	35.4	97.6	886	Jan. 1945—Dec. 1962	6534
Greensboro, N.C.	36.1	80.0	1304	Nov. 1945—Dec. 1962	6184

The computing routine included the correction for linear change from midnight to midnight. This harmonic analysis gives the periods of 24, 12, 8, and 6 solar hours. The determination of the lunar semidiurnal oscillation was then performed following the method developed by Chapman and Miller[5] and also described by Tschu[13]. For the two Puerto Rican stations San Juan and Aguadilla, the original data were obtained from the NWRC on magnetic tape, and all calculations for these stations, including the computations of the bi-hourly mean values and the correction for linear change, were performed at NCAR on a CDC 3600 computer, because this permitted greater flexibility in experimenting with the data, especially as far as the omission of days with greater variability of the pressure was concerned.

At all six stations one or more changes in the observing routine occurred: At Aguadilla, for instance, the observations were made 30 min. past the hour from 1941 through 1952, on the hour from 1954 on. In all these cases, the data have been divided into time intervals of uniform observations practice. The various tidal determinations have been made separately for these time intervals. Then, after the appropriate corrections of the phase constants were made, the results for the two time intervals were combined.

After the determination of the tides for the six stations was completed, some errors in the card deck for the lunar integers L were discovered. During August 1942 all the lunar numbers were too small by 3, and in the period from 1943 to 1960, 18 days were assigned the wrong lunar number, but only in five instances was the difference between the correct and incorrect number greater than 1.

For San Juan and Aguadilla the analysis was repeated with the corrected lunar deck. Table 2 shows for Aguadilla the effect of, or rather the absence of an appreciable effect, of the errors in the lunar deck. The lunar tidal oscillation is given in the customary form.

$$L_2(p_0)=l_2 \sin(30t+\lambda_2)$$

where t is local mean lunar time, l_2 the amplitude expressed in microbars ($1\ \mu b.=10^{-3}$ mb.$=1$ gm. cm.$^{-1}$ sec.$^{-2}$), λ_2 the phase constant in degrees. The radius of the probable error circle is denoted by r. The results are given separately for the time intervals I (1941–1953) and II (1954–June 1958) into which the data are separated for the computation in order to allow for the change in observing time mentioned previously. Only the harmonic constants for the three seasons, but not those for the annual means are given, because any differences due to a faulty lunar deck should show up most in the results based on less material. The first line in the table for each period gives the results obtained before elimination of the errors in the lunar deck, the second line the results with the correct deck. The data, and those for San Juan, have been analyzed under the further restriction that those days were eliminated on which the pressure during any 2-hour interval changed by more than 4 mb. As would be expected for tropical stations, very few days were eliminated because of this restriction. The results with this restriction are shown in the third line for each of the two time intervals. A comparison of the appropriate results shows that the deck errors, as well as the 4-mb. restriction, gave results which are not different from those obtained with the corrected deck. It seemed, therefore, not necessary to recompute the lunar tide for the other stations with the corrected deck or to introduce the 4-mb. restriction for the other stations. However, the results for Aguadilla and San Juan given in table 3 are computed with the corrected lunar deck.

A somewhat surprising feature is the large value of l_2 during the D season for the time interval II at Aguadilla. If d is the distance between two points representing two oscillations in a polar diagram, e^2 the sum of the squares of the probable errors of the two determinations, then $2^{-d^2/e^2}$ is the probability that such a separation between the oscillations is due to pure chance, as shown by Bartels [1]. In the present case, this probability is 1:4 so that one might well expect to find such a difference accidentally. Actually, because of the limited number of data available for the determination, the probability is even higher than indicated by the test which assumes a very large number of data. It will also be noted that the probable-error circle during the second time interval is larger than one would expect from its value during the first time interval and allowing for the difference in the length of the time intervals.

TABLE 2.—*Comparison of lunar tidal computation for Aguadilla*

	D Season			*J* Season			*E* Season			Length of Record
	l_2 (μb.)	λ_2 (deg.)	r (μb.)	l_2 (μb.)	λ_2 (deg.)	r (μb.)	l_2 (μb.)	λ_2 (deg.)	r (μb.)	
Period I										
Deck error	43.6	49	4.4	54.9	74	5.8	51.0	77	6.1	1941-53
No error	43.6	49	4.4	56.7	75	5.5	51.0	77	6.1	13 yr.
4-mb. restriction	43.2	49.9	4.0	57.0	76.4	5.6	49.7	76.8	6.5	
Period II										
Deck error	60.4	44	12.4	48.9	76	9.5	35.3	71	7.9	1954-June '58
No error	60.6	44	12.2	48.6	74	9.8	36.7	73	7.7	4.5 yr.
4-mb. restriction	60.6	44.3	12.2	48.6	74.4	9.8	37.0	78.4	6.9	

TABLE 3.—*Lunar semidiurnal pressure oscillation*

Station	Season	l_2 (μb.)	λ_2 (deg.)	r (μb.)
Balboa, Panama	Ann.	58.3	77.0	2.9
	D	45.7	52.9	4.1
	J	72.0	83.8	5.9
	E	60.3	84.7	5.6
San Juan, P.R.	Ann.	50.7	75.2	2.1
	D	43.0	52.9	4.1
	J	61.3	84.3	3.5
	E	52.9	82.2	3.8
Aguadilla, P.R.	Ann.	48.4	68.7	2.7
	D	47.7	49.1	4.9
	J	54.7	77.0	4.9
	E	46.4	78.2	4.6
Burbank, Calif.	Ann.	25.8	64.0	3.3
	D	18.4	14.0	7.2
	J	36.7	74.2	4.6
	E	30.0	80.4	4.8
Oklahoma City, Okla.	Ann.	24.3	70.4	8.4
	D	20.5	83.7	14.7
	J	28.5	66.4	11.8
	E	24.3	73.8	10.2
Greensboro, N.C.	Ann.	36.1	78.3	5.1
	D	39.4	68.5	14.1
	J	39.8	85.7	4.4
	E	30.2	82.3	7.6

2. THE LUNAR SEMIDIURNAL TIDE

The results of the lunar tidal determinations are shown in table 3 which gives the amplitude l_2, the phase angle λ_2, and the radius of the probable error circle r. In general, the annual mean amplitude shows the well-known decrease with distance from the equator. The amplitude is higher at Greensboro, N.C. than at Oklahoma City and at Burbank, Calif., which indicates the westward decrease of the amplitude over the United States found previously by Chapman and Westfold [6].

The seasonal variation of the lunar semidiurnal tide is generally characterized by a smaller phase constant (later high tide) during the D months than in the other two seasons. This is also shown by the data presented in table 3, with the exception of Oklahoma City. But here the radii of the probable error circles are so large that little if any weight can be given to this anomaly. The angle between the line from the origin to the point in the harmonic dial representing the oscillation and the tangent to the error circle is $\sin^{-1}(r/l_2)$ so that the phase constant for the D months at Oklahoma City may be given as $84°\pm46°$, showing clearly that the lunar tide is not well determined.

Another feature of the seasonal variation of the lunar tide is the maximum amplitude during the J months which is shown at all stations given in table 3, although at some stations with large probable errors, the difference between the D and J months is statistically not significant.

In considering the data in table 3, it should be remembered that the determination of an oscillation cannot be considered satisfactory if the amplitude is not at least three times larger than the radius of the probable error circle. The probable error circle is commonly used in considering the reliability of the determinations of geophysical periodicities, largely thanks to the pioneering efforts of Bartels. It could, of course, be replaced by some other statistical measure. However, the use of the probable error makes the comparison with earlier results much easier and permits also the direct application of various theorems derived for it to the interpretation of the results.

TABLE 4.—*Probability of large amplitudes in random data*

A/r	$m=12$	$m=\infty$
0.5	1: 1.2	1: 1.2
1	1: 1.9	1: 2.0
1.5	1: 3.9	1: 4.7
2	1: 9.4	1: 15.8
2.5	1: 23.8	1: 74.4
3	1: 61	1: 493
3.5	1: 146	1: 4870
4	1: 324	1:59900
4.5	1: 652	$1:1.11\cdot10^6$
5	1: 1200	$1:29.4\cdot10^6$
6	1: 3290	
7	1: 8100	
8	1:12200	
9	1:19700	
10	1:26900	

If the amplitude A, the radius of the probable error circle r, and the number of groups of data from which the probable error circle was computed are known, the probability p can be estimated that an amplitude of this magnitude may be found in random data (Haurwitz [7]). This probability p is shown in table 4 for $m=12$, and for $m=\infty$. The number 12 was selected because the Chapman-Miller method used here is in effect based on the determination of the lunar tide L_2 by means of the solar semidiurnal oscillation S_2 grouped into 12 lunar phase groups. If $A=3r$, the probability that such an amplitude is found in random data is 1:60, but this probability decreases rapidly as A increases relative to r. Table 4 should help in the understanding of the significance of the probable-error circle in connection with the presentation of geophysical oscillations.

While the amplitudes of the lunar tide at San Juan and Aguadilla agree reasonably well, the phase angles differ by about 7° despite the close proximity of the stations. Similar phase angle differences will be found for the solar-day oscillations at both stations (table 5). Since allowance has been made for the fact that the observations were not all made on the hour, the explanation cannot be sought in a change of the observing routine, and in fact no explanation is readily apparent. Correspondence with the National Weather Records Center on this point indicated that some minor changes may have been made in the times when the observations were taken, but it is not possible to reconstruct such hypothetical changes now.

It is of some interest to mention here briefly some results of a pilot study undertaken prior to the determination of lunar tides on a large scale. In order to have a statistical estimate of how many data might be required for a reliable determination of the lunar tide an analysis was performed using the pressure observations at Balboa for the year 1953. The lunar tidal pressure oscillation was found to be:

$$44.8\ \mu\text{b. sin}\ (30t+84.8°),$$

TABLE 5.—*Solar-day oscillations*

Station	Season	s_1 (μb.)	σ_1 (deg.)	r_1 (μb.)	s_2 (μb.)	σ_2 (deg.)	r_2	s_3 (μb.)	σ_3 (deg.)	r_3 (μb.)	s_4 (μb.)	σ_4 (deg.)	r_4 (μb.)
Balboa	Ann.	651.2	7.5		1286.2	153.4		47.7	49.8		41.4	172.0	
	D	684.6	8.2	6.8	1370.8	157.3		80.4	29.5	3.4	48.1	182.1	3.0
	J	520.0	9.4	8.5	1153.3	148.2		36.5	106.3	5.4	20.3	150.9	6.2
	E	749.9	5.4	8.0	1352.4	154.2		47.4	52.0	3.9	58.1	170.8	3.4
San Juan	Ann.	281.1	353.4		1045.1	149.7		47.5	48.9		47.6	166.5	
	D	300.8	341.8	7.6	1127.7	152.4		170.5	10.1	2.8	68.0	191.8	2.9
	J	235.3	11.4	7.8	899.4	146.0		99.6	163.1	3.3	36.8	137.6	2.2
	E	325.3	351.2	7.4	1112.7	149.9		54.1	63.3	2.7	50.6	154.6	2.8
Aguadilla	Ann.	272.1	336.4		1046.3	146.5		77.5	32.2		45.1	155.6	
	D	309.4	334.0	8.1	1170.9	149.7		190.3	2.9	2.2	60.4	177.3	2.6
	J	205.7	348.0	5.2	878.0	142.0		74.8	131.1	2.4	34.4	133.1	2.4
	E	307.4	331.1	7.3	1096.3	146.8		81.8	44.4	3.2	48.4	144.6	2.1
Burbank	Ann.	720.0	358.2		725.5	150.0		88.9	16.4		30.6	226.9	
	D	686.6	1.8	12.1	835.7	155.8		272.7	357.6	4.2	88.0	202.0	2.7
	J	715.2	350.8	8.8	604.4	142.1		99.9	144.1	3.0	19.0	297.1	2.4
	E	703.3	357.8	9.6	746.4	150.2		69.3	23.1	3.2	17.7	300.0	1.9
Oklahoma City	Ann.	818.7	339.7		693.8	148.4		55.5	3.5		56.6	193.1	
	D	590.8	346.6	29.9	728.7	156.0		244.4	351.3	11.6	108.2	185.3	11.5
	J	997.5	335.2	19.7	625.7	138.2		130.9	149.4	7.6	46.8	196.8	11.3
	E	868.8	340.3	22.2	742.9	149.1		107.2	211.4	9.0	20.8	227.3	7.4
Greensboro	Ann.	664.0	345.3		734.8	158.5		78.6	4.4		27.3	184.0	
	D	502.8	350.9	25.6	744.2	165.2		256.0	356.8	12.3	83.6	207.7	11.4
	J	752.7	339.0	11.6	694.5	150.0		78.1	156.6	3.9	23.9	110.5	2.8
	E	744.9	347.7	19.7	778.1	158.7		48.7	358.9	4.4	8.5	85.3	4.3

with a radius of the probable error circle of 12.3 μb. Since the error decreases inversely proportional to the square root of the number of observations one should expect for 17.5 yr. of data a probable error of 2.95 μb., very close to the value given in table 3. It is also interesting to note that a determination of the lunar tide from one day's data could be expected to have a probable error of about 230 μb.

3. THE SOLAR-DAY OSCILLATIONS

The harmonic constants for the solar-day oscillations with periods of $1/n$ mean solar days, $n=1,2,3,4$, are given in table 5 for the annual means, and for the three seasons in the form

$$S_n(p_0)=s_n \sin(15\ nt+\sigma_n)$$

where s_n and σ_n are amplitude and phase constant of the nth oscillation, S_n, and t mean solar time in hours. Since the data had to be grouped according to the lunar phase integer for the computation of L_2 the solar-day oscillations were determined first for these 12 groups. Table 5 gives the mean values of the harmonic constants for these 12 groups and the radii of the probable error circles for these means as computed from the grouping. In the case of the solar semidiurnal oscillation the errors computed in this manner would be too large because they would contain the effect of the lunar tide. The errors given in table 3 for the lunar tide are actually the residual errors applying both to the solar and lunar semidiurnal oscillations. They are not repeated in table 5. No errors are given for the annual means of the solar oscillations in table 5. They are comparable to the errors for the seasonal values.

The solar 24-hour oscillation S_1 is known to be irregularly distributed over the earth. In table 5 the two stations on the island of Puerto Rico show a much smaller amplitude than the other stations. The pressure maximum occurs about 5:30 a.m. at Balboa, but in general between 6:00 and 8:00 a.m. at the other stations. An analysis of the global distribution of this oscillation (strictly speaking, its annual mean) had shown that the worldwide maximum, freed of local influences, occurs at 5:00 a.m. approximately [8]. The data of table 5 show a seasonal variation of S_1, but this variation is not uniform.

The solar semidiurnal oscillation S_2 shows the well-known decrease with increasing latitude, although this decrease is not quite regular, as shown in table 5 by Greensboro in the eastern part of the United States. It had already been noted by Spar [12] that the amplitudes are large along the east coast of the United States. All stations have their minimum amplitude in summer, another well-known characteristic of the semidiurnal oscillation.

The main term of the 8-hour solar oscillation S_3 is characterized by a phase shift of 180° from one solstice to the next (for instance, [11]). Since the latitude dependence of the amplitude of S_3 is mainly proportional to the associated Legendre functions $P_4^3(\varphi)$ where φ is the latitude, it has its maximum at 30° N. and S. Another term, about ⅓ as large, and without such a pronounced annual variation, has its maximum at the equator. Accordingly, it is seen in table 5 that the most southerly stations have a smaller phase shift from summer to winter than the stations at higher latitudes. The maximum amplitude occurs during the winter months, another well established feature of this oscillation.

The 6-hour solar oscillation S_4 has lately been studied by Kertz [9] who combined all the earlier data and computed some additional ones. Its main term is characterized by the associated Legendre function $P_5^4(\varphi)$ with a maximum amplitude around 25° latitude and with a pronounced seasonal variation. The harmonic parameters in table 5 show such a strong seasonal variation, and, except for Balboa, a maximum amplitude during the D months, in agreement with Kertz's result for the term with $P_5^4(\varphi)$

The peculiar phase differences of the solar-day oscillations at San Juan and Aguadilla have already been commented on in connection with the lunar tide.

ACKNOWLEDGMENTS

Our thanks are due to the Director and staff of the National Weather Records Center who furnished the data for this work, performed many of the preliminary calculations, and patiently answered our many inquiries.

REFERENCES

1. J. Bartels, "Statistical Methods for Research on Diurnal Variations," *Terrestrial Magnetism and Atmospheric Electricity*, vol. 37, No. 3, 1932, pp. 291–302.
2. J. Bartels, "A Table of Daily Integers, 1902–1952, Seasonal, Solar, Lunar, and Geomagnetic," *Scientific Report* No. 2 on contract AF 19(604)-503, Geophysical Institute, University of Alaska, 1954, 18 pp.
3. J. Bartels and G. Fanselau, "Geophysikalischer Mond-Almanach," *Zeitschrift für Geophysik*, vol. 13, 1937, pp. 311–328.
4. G. W. Brier, "Diurnal and Semidiurnal Atmospheric Tides in Relation to Precipitation Variations," *Monthly Weather Review*, vol. 93, No. 2, Feb. 1965, pp. 93–100.
5. S. Chapman and J. C. P. Miller, "The Statistical Determination of Lunar Daily Variations in Geomagnetic and Meteorological Elements," *Monthly Notices, Royal Astronomical Society, Geophysical Supplement*, vol. 4, No. 9, May 1940, pp. 649–669.
6. S. Chapman and K. C. Westfold, "A Comparison of the Annual Mean Solar and Lunar Atmospheric Tides in Barometric Pressure, As Regards Their Worldwide Distribution of Amplitude and Phase," *Journal of Atmospheric and Terrestrial Physics*, vol. 8, No. 1/2, Feb. 1956, pp. 1–23.
7. B. Haurwitz, "Tidal Phenomena in the Upper Atmosphere," *WMO Technical Note* No. 58 (WMO No. 146.TP. 69) World Meteorological Organization, 1964, 26 pp.
8. B. Haurwitz, "The Diurnal Surface-Pressure Oscillation," *Archiv für Meteorologie, Geophysik und Bioklimatologie*, Ser. A, 1965 (in press).
9. W. Kertz, "Partialwellen in den halb- und vierteltäglichen gezeitenartigen Schwingungen der Atmosphäre," *Archiv für Meteorologie, Geophysik und Bioklimatologie*, Ser A, vol. 11, No. 1, 1959, pp. 48–63.
10. I. A. Lund, "Indications of a Lunar Synodical Period in United States Observations of Sunshine," *Journal of the Atmospheric Sciences*, vol. 22, No. 1, Jan. 1965, pp. 24–39.
11. M. Siebert, "Atmospheric Tides," *Advances in Geophysics*, vol. 7, Academic Press, 1961, pp. 105–182.
12. J. Spar, "Characteristics of the Semidiurnal Pressure Wave in the United States," *Bulletin of the American Meteorological Society*, vol. 33, No. 10, Dec. 1952, pp. 438–441.
13. K.-K. Tschu, "On the Practical Determination of Lunar and Luni-Solar Daily Variations in Certain Geophysical Data," *Australian Journal of Scientific Research*, Ser. A, vol. 2, No. 1, Mar. 1949, pp. 1–24. (See also: S. Chapman, "The Calculation of the Probable Error of Determinations of Lunar Daily Harmonic Component Variations in Geophysical Data: A Correction," *Australian Journal of Scientific Research*, Ser. A, vol. 5, No. 1, Mar. 1952, pp. 218–222.)

[*Received May 4, 1965*]

Nicht im Handel

Reprint from

Archiv für Meteorologie, Geophysik und Bioklimatologie

Serie A: Meteorologie und Geophysik, Band 14, Heft 4, 1965

Herausgegeben von

Doz. Dr. W. Mörikofer, Davos, und Prof. Dr. F. Steinhauser, Wien

Springer-Verlag in Wien

551.543.1

(National Center for Atmospheric Research, Boulder, Colorado)

The Diurnal Surface-Pressure Oscillation

By

B. Haurwitz

With 5 Figures

(Received February 18, 1965)

Summary. A spherical harmonic analysis of the diurnal surface pressure oscillation shows that its main part can be represented by a wave travelling westward with the sun. The amplitude of this wave is about half of that of the semidiurnal oscillation [eq. (7)]. For the discussion of the excitation of the diurnal oscillation the equivalent depths (Table 4) and Hough functions (Table 5, 6) for the three lowest symmetrical modes are computed. There is no difficulty in accounting for the smallness of the diurnal oscillation compared to the semidiurnal oscillation on the basis of thermal excitation, even if the semidiurnal oscillation is not greatly magnified by resonance.

Zusammenfassung. Die sphärische harmonische Analyse der 24stündigen Bodenluftdruckschwankung zeigt, daß ihr Hauptteil durch eine mit der Sonne westwärts wandernde Welle dargestellt werden kann. Die Amplitude dieser Welle ist ungefähr die Hälfte der 12stündigen Schwankung [Gleichung (7)]. Zur Diskussion der thermischen Erregung der 24stündigen Schwankung wurden die äquivalenten Tiefen (Tabelle 4) und Hough-Funktionen (Tabellen 5, 6) für die drei niedrigsten symmetrischen Typen berechnet. Es besteht keine Schwierigkeit, auf Grund der Theorie der thermischen Erregung zu erklären, warum die 24stündige Schwankung viel kleiner ist als die 12stündige, selbst wenn die letztere nicht bedeutend durch Resonanz vergrößert wird.

Résumé. L'analyse harmonique sphérique des variations de pression au sol en 24 heures montre que sa partie principale peut être représentée par une onde se propageant vers l'ouest avec le soleil. L'amplitude de cette onde est d'à peu près la moitié de la variation en 12 heures [équation (7)]. Pour la discussion de la stimulation thermique de la variation en 24 heures, on a calculé les dépressions équivalentes (tableau 4) ainsi que les fonctions de Hough (tableaux 5 et 6) et cela pour les trois types de symétrie les plus bas. En se basant sur la théorie de la stimulation thermique, il n'est pas difficile d'ex-

pliquer pourquoi les variations en 24 heures sont beaucoup plus faibles que celles se produisant en 12 heures, même si ces dernières ne sont pas notablement renforcées par des effects de résonance.

I. Introduction

The daily[1] variation of the atmospheric surface pressure when freed of the irregular meteorological noise has a pronounced semidiurnal period whose amplitude is generally considerably larger than that of the diurnal oscillation. Further, the semidiurnal surface pressure oscillation, $S_2(p_0)$, is very uniformly distributed over the earth. In contrast, the diurnal pressure oscillation, $S_1(p_0)$, shows a rather irregular geographical distribution which is much influenced by topography and surface conditions. It is clear that geographically caused phenomena with a daily period such as mountain and valley winds or sea and land breezes must have a larger effect on the diurnal than on the semidiurnal pressure oscillation. But these circulations affect only a relatively small part of the earth and can hardly account for the world-wide difference between $S_1(p_0)$ and $S_2(p_0)$, especially for the fact that the latter oscillation has a larger amplitude than $S_1(p_0)$.

It is well known that the so-called "resonance theory," first suggested by KELVIN [*12*], attributed the large size of $S_2(p_0)$ compared to both $S_1(p_0)$ and the lunar semidiurnal pressure oscillation, to a free period of the terrestrial atmosphere which is so close to 12 solar hours that a magnification of 60 or more times results. The existence of such a free period seemed likely according to theoretical studies (for instance PEKERIS, [*16*]) as long as it could be assumed that the stratopause at about 50 km altitude has a temperature of around 350° K. But rocket measurements have established that the temperatures here are much lower than required for strong resonance magnification so that the large amplitude of $S_2(p_0)$ cannot be explained in this manner.

To overcome this difficulty SEN and WHITE [*20*] and SIEBERT [*21*] have pointed out almost simultaneously that earlier theories of the thermal excitation of atmospheric oscillations have considered only atmospheric heating by turbulent transfer from the ground upward while in fact the atmosphere is also heated by direct absorption of incoming solar radiation. The latter will affect the whole mass of the atmosphere, not only its lowest 10 percent or less, as turbulent heat transfer does. In this manner, and especially since some of the higher layers of the atmosphere, such as the ozone layer considered by BUTLER and SMALL [*1*], must undergo strong daily temperature variations because of their radiative properties, the available generating forces are greatly increased. Consequently, the resonance magnification required becomes much smaller, and the existence of a free period in close proximity to that of the generating force need no longer be postulated.

[1] The total variation of a meteorological parameter throughout the solar day is here referred to as "daily," with its harmonic components a 24-hourly or diurnal, S_1, 12-hourly or semidiurnal, S_2, etc. The letter S_n and its first (or only) subscript denote an oscillation which is the nth part of a solar day. When required the parameter considered is added in parenthesis. A superscript indicates the wave number. Thus $S_1^1(p_0)$ stands for that part of the solar diurnal pressure oscillation represented by one wave around the earth's circumference. The global distribution of such a wave can be expressed by a series of associated Legendre functions (or for theoretical considerations more appropriately by Hough functions, see Section 4).

If this explanation of the semidiurnal oscillation is accepted, the smallness of the diurnal oscillation has to be explained, because in the daily temperature curve the diurnal harmonic has a considerably larger amplitude than the semidiurnal harmonic. Since no systematic study has been made of the diurnal pressure wave as a world-wide feature, it has not been possible to state just how much larger the semidiurnal planetary pressure wave is than the diurnal wave.

The present paper is an attempt to fill this gap by presenting an analysis of the geographical distribution of the diurnal surface pressure oscillation and its representation by spherical harmonics, similar to the procedure followed for the semidiurnal pressure oscillation (HAURWITZ [*9*]). This representation of the diurnal pressure wave with its great local variations will only give the broadest features of this oscillation unless very many terms in the harmonic series are computed. But a few terms should suffice since we are interested here in what may be called the "planetary" pattern of the diurnal pressure oscillation, that is the broad global features produced by the daily heating and the large-scale distribution of water and land rather than the superimposed local peculiarities.

It is pertinent to make reference here to a paper by SOLBERG [*23*] in which the quasistatic assumption of the tidal theory is criticized, that is the assumption of hydrostatic equilibrium in the vertical. According to SOLBERG's investigation this simplification is at least questionable for periods longer than twelve hours. It is beyond the scope of this paper to consider this problem, and wherever necessary the results of the quasistatic tidal theory will be used here.

II. Data

The analysis is based on data largely taken from publications by HANN (mainly [*5*] but also [*6, 7, 8*]). Some stations in northern Europe have been studied by SCHOU [*18*]. A few data for Malaya are given by FROST [*4*]. SELLICK [*19*] has published some analyses for southern Africa. In a few instances more than one analysis result was available for a station. In such cases the analysis based on the longer record was always chosen. This applies in particular to some Canadian stations for which the diurnal pressure oscillation was determined incidentally to a computation of the 12-hourly lunar air tide by CHAPMAN [*2*] and to Accra (CHAPMAN [*3*]). Of particular help in filling out a gap over the Northern Atlantic Ocean was a paper by ROSENTHAL and BAUM [*17*] which dealt with weathership observations. Unfortunately nothing like this exists over the Pacific Ocean.

Because of the nature of the available material the radius of the probable-error circle, or another statistical measure for the reliability of the individual determination of the diurnal pressure waves is not available. In general, only data based on at least five years' observations have been used, but for some high-latitude stations it was necessary to include

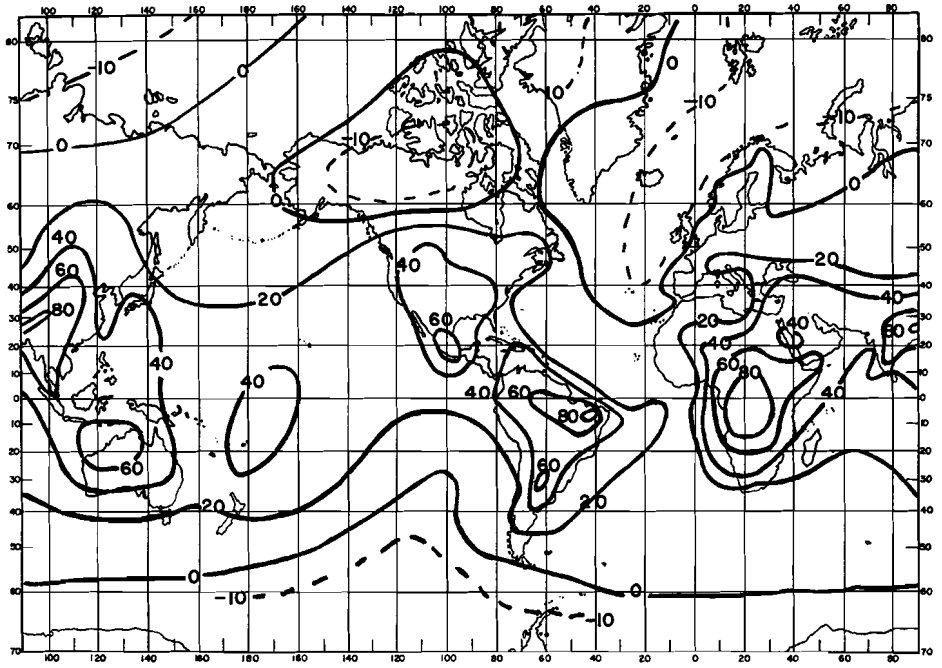

Fig. 1. Factor of the cosine term of the diurnal pressure oscillation. Unit 10^{-2} mm Hg

results of only one year's observations. Since in the harmonic analysis the various latitudes are weighted according to their area, any errors due to inaccuracies of the harmonic coefficients for high latitudes will be small.

Table 1. *Distribution of Stations*

Latitude	No. of Stations	Latitude	No. of Stations
0°—10° N	9	0°—10° S	13
10 —20	10	10 —20	23
20 —30	13	20 —30	10
30 —40	31	30 —40	9
40 —50	54	40 —50	1
50 —60	32	50 —60	2
60 —70	11		
70 —90	10		

Any uncertainties in the planetary diurnal pressure oscillations are much more likely caused by geographic effects on the oscillations than by too short a series of data.

Altogether 228 stations are available. Unfortunately, the distribution of these stations is very far from uniform as can be seen from Table 1.

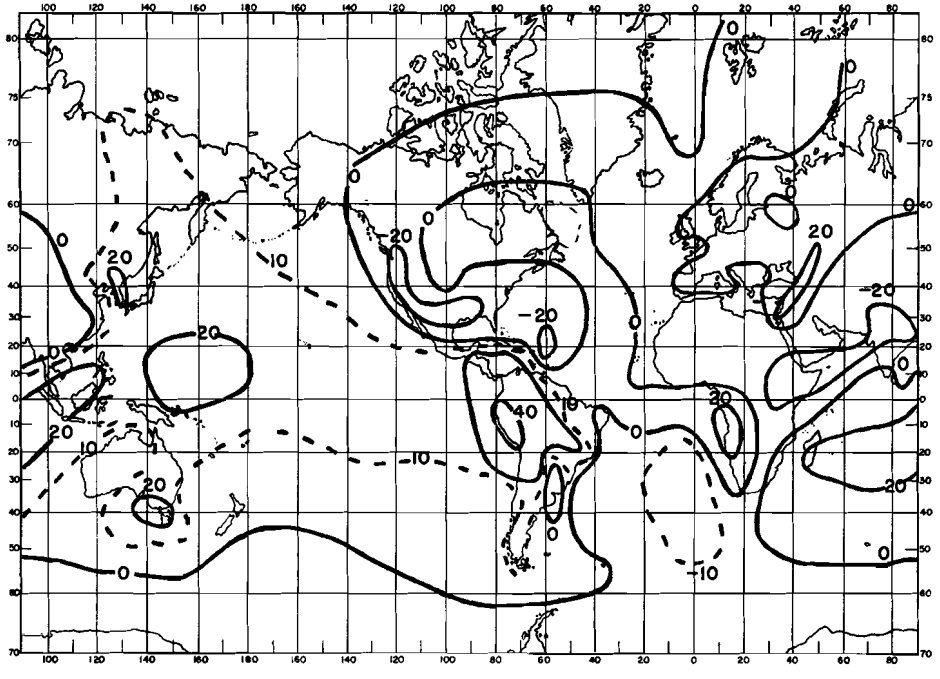

Fig. 2. Factor of the sine term of the diurnal pressure oscillation. Unit 10^{-2} mm Hg

More than half the available stations are situated in middle latitudes of the Northern Hemisphere, between 30° and 60° N. Moreover, in this latitude belt they are mainly concentrated in Europe and North America.

The diurnal pressure oscillation is given in one of the two forms (t' = local mean time in degrees)

$$S_1 = a \sin (t' + \alpha) = p \cos t' + q \sin t' \qquad (1)$$

For the spherical harmonic analysis the harmonic coefficients p and q have to be used. These coefficients were plotted on large-scale maps for each available station, and isopleths of the p and q were drawn, disregarding those stations which are clearly disturbed because of their location. These maps are shown as Fig. 1 and 2. On the original working maps the isopleths of p and q are drawn for intervals of 0.1 mm Hg while in the Figures reproduced here an interval 0.2 mm Hg has been used to allow greater reduction in size of the Figures. The distribution of the diurnal pressure

oscillation is clearly less regular than that of the semidiurnal oscillation. Nevertheless, one can recognize that the diurnal pressure oscillation, by and large, decreases polewards from the equator. Also it is very strongly influenced by the distribution of water and land, with the land having much larger values than the oceans, as expected in view of the similar behavior of the diurnal temperature wave.

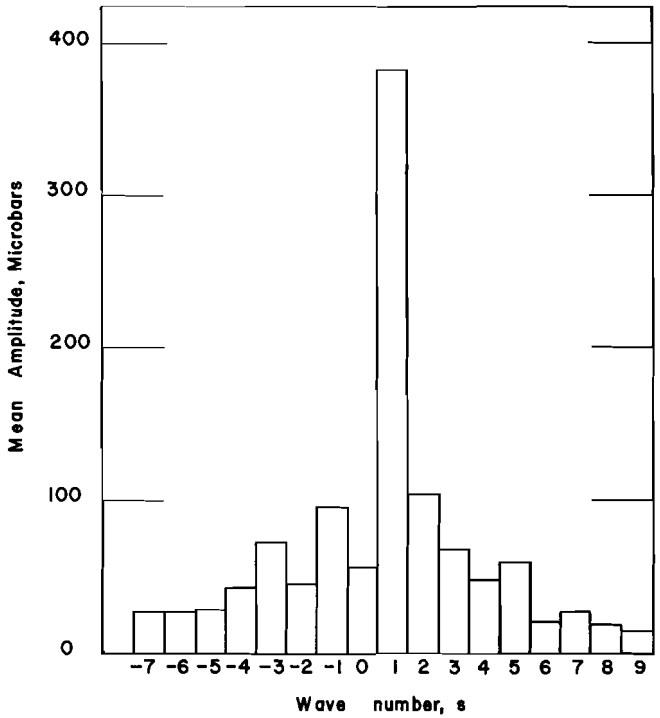

Fig. 3. Component waves of the diurnal pressure oscillation

The values of the p and q for grid points 15° of longitude apart, starting with the Greenwich meridian and for every tenth degree of colatitude extending from 10° to 140° colatitude were read off these maps and used for the harmonic analysis.

III. Harmonic Analysis

For the representation of the diurnal pressure oscillation we require first a development of the harmonic coefficients p and q at a given colatitude by trigonometric series in λ, the longitude. Let

$$p = \sum_{\nu} (k_\nu \cos \nu\lambda + l_\nu \sin \nu\lambda)$$
$$q = \sum_{\nu} (m_\nu \cos \nu\lambda + n_\nu \sin \nu\lambda) \qquad (2)$$

The integer ν goes from zero to 12 in our case since 24 grid points are available for each latitude circle.

If the eq. (2) are substituted into (1) it follows with the introduction of Greenwich Mean Time, t, (in degrees),

$$t = t' - \lambda$$

and with the aid of some trigonometric formulae that

$$S_1 = \tfrac{1}{2} \sum_{\nu} \{(k_\nu - n_\nu) \cos [t + (\nu + 1)\lambda] + (k_\nu + n_\nu) \cos [t - (\nu - 1)\lambda]$$
$$+ (m_\nu + l_\nu) \sin [t + (\nu + 1)\lambda] + (m_\nu - l_\nu) \sin [t - (\nu - 1)]\} \qquad (3)$$

as shown by KERTZ [*14*].

Thus the wave which moves around the earth with the (mean) sun has the coefficients k_0 and m_0, as is immediately clear from (3). In addition to this wave there may be others with wave numbers different from one. Negative wave numbers mean that the wave moves in the direction opposite to the sun, from west to east. The reason for the appearance of all these waves is the influence of the irregular distribution of water and land with its effect on the distribution of the diurnal temperature wave. Eq. (3) shows that the harmonic coefficients of the various component waves of $S_1(p_0)$ can be computed according to the following scheme (after KERTZ [*14*]).

s	c_s Factor of $\cos(t + s\lambda)$	s_s Factor of $\sin(t + s\lambda)$
	...	...
−3	$\frac{1}{2}(k_4 + n_4)$	$\frac{1}{2}(m_4 - l_4)$
−2	$\frac{1}{2}(k_3 + n_3)$	$\frac{1}{2}(m_3 - l_3)$
−1	$\frac{1}{2}(k_2 + n_2)$	$\frac{1}{2}(m_2 - l_2)$
0	$\frac{1}{2}(k_1 + n_1)$	$\frac{1}{2}(m_1 - l_1)$
1	k_0	m_0
2	$\frac{1}{2}(k_1 - n_1)$	$\frac{1}{2}(m_1 + l_1)$
3	$\frac{1}{2}(k_2 - n_2)$	$\frac{1}{2}(m_2 + l_2)$
4	$\frac{1}{2}(k_3 - n_3)$	$\frac{1}{2}(m_3 + l_3)$
	...	...

With these formulae the cosine and sine factors, c_s and s_s of the different waves have been determined for wave numbers $-7 \leqq s \leqq +9$. In order to obtain an estimate of the magnitudes of the component waves of $S_1(p_0)$ we have computed the amplitudes for each wave of number s and for each colatitude $\vartheta_r = 10°, 20°, \ldots, 130°, 140°$

$$[a_s(\vartheta_r)]^2 = [c_s(\vartheta_r)]^2 + [s_s(\vartheta_r)]^2$$

From these amplitudes for the 14 colatitude circles a mean amplitude $\bar{a}_s$ for each wave number s was computed by

$$\bar{a}_s = \left\{\sum_r a_s(\vartheta_r) \sin \vartheta_r\right\} \Big/ \left\{\sum_r \sin \vartheta_r\right\} \qquad (4)$$

The factor $\sin \vartheta_r$ has been added here to allow for the areas of the different latitude belts. The results of the computation are shown in Fig. 3 where the unit of pressure is the microbar, $1\ \mu b = 10^{-3}$ mbar.

As would be expected the wave with one maximum and minimum which moves around the earth with the same speed as the sun has by far the largest amplitude. The next largest waves are those with wave numbers 2 and — 1. There is also a small standing oscillation, $s = 0$, but it is less significant than some of the waves with larger absolute wave numbers. Nevertheless, this wave together with the three largest waves $s = 1, 2, -1$ has been included in the further analysis because of its possible theoretical interest.

The next step in the spherical harmonic analysis is the representation of the harmonic coefficients $c_s(\vartheta)$ and $s_s(\vartheta)$ by series of associated Legendre functions of appropriate degree s,

$$\left.\begin{matrix} c_s(\vartheta_r) \\ s_s(\vartheta_r) \end{matrix}\right\} = \sum_{i=0}^{2} \left\{\begin{matrix} f^{|s|}_{|s|+i} \\ g^{|s|}_{|s|+i} \end{matrix}\right\} P^{|s|}_{|s|+i}(\vartheta_r) \tag{5}$$

As indicated by (5) only three terms will be used for the representation of each component wave. The coefficients f and g are determined by the method of least squares, and the data have been, as customary, weighted by the factor $\sin\vartheta_r$ to allow for the areas of the different latitude belts. Thus it is required that

$$M = \sum_r [c_s(\vartheta_r) - f^{|s|}_{|s|} P^{|s|}_{|s|}(\vartheta_r) - f^{|s|}_{|s|+1} P^{|s|}_{|s|+1}(\vartheta_r) - f^{|s|}_{|s|+2} P^{|s|}_{|s|+2}(\vartheta_r)]^2 \sin\vartheta_r$$

and a corresponding expression involving $s_s(\vartheta_r)$ are made minima by the proper choice of the $f^{|s|}_{|s|+i}$ and $g^{|s|}_{|s|+i}$. It must be pointed out that the orthogonality of the associated Legendre functions could not be used in these calculations because the available data extend only through part of the Southern Hemisphere. Consequently if more terms are to be taken in the series (5) the earlier coefficients have to be recomputed.

We shall write

$$\left[f^{|s|}_{|s|+i}\cos(t+s\lambda) + g^{|s|}_{|s|+i}\sin(t+s\lambda)\right] P^{|s|}_{|s|+i} = B^{|s|}_{|s|+i} P^{|s|}_{|s|+i}\sin\left(t+s\lambda+\beta^{|s|}_{|s|+i}\right). \tag{6}$$

The results of the harmonic analysis of the diurnal surface pressure oscillation are given in Table 2.

Table 2 shows like Fig. 3 that despite the great irregularities of the geographical distribution of the diurnal pressure oscillation a wave moving westward with the sun is clearly predominant. In this oscillation the symmetrical terms with P^1_1 and P^1_3 are the largest. Since their phase constants differ by nearly 180° the two terms can be combined as follows

$$S^1_1(p_0) = 464\ \mu b\,[P^1_1(\vartheta) - 0.453\,P^1_3(\vartheta)]\sin(t+\lambda+12°) \tag{7}$$

which can also be well approximated by

$$S^1_1(p_0) = 593\ \mu b\sin^3\vartheta\sin(t+\lambda+12°) \tag{8}$$

As in the case of the semidiurnal pressure oscillation the empirical latitude distribution is well represented by the third power of the cosine of the latitude indicating a rapid decrease of the amplitude with the distance from the equator. The amplitude distributions for $S^1_1(p_0)$, given by the amplitudes and phase constants of Table 2 and by (8) are represented in Fig. 4 by curves 1 and 2, respectively. The crosses indicate the actual amplitudes of $S^1_1(p_0)$ for each tenth degree of latitude. Since the directly determined phase angles for 10° and 20° colatitude are 142° and 156°, these two values are here shown as negative. Curve 3 will be discussed in the next Section.

Table 2. *Harmonic Constants of the Diurnal Surface Pressure Oscillation*

Wave Type $S^s_1(P_0)$	$\lvert s\rvert+i$	Amplitude (microbar) $B^{\lvert s\rvert}_{\lvert s\rvert+i}$	Phase constant $\beta^{\lvert s\rvert}_{\lvert s\rvert+i}$
$S^1_1(p_0)$	1	464	12°
	2	69	321
	3	210	195
$S^2_1(p_0)$	2	158	263
	3	69	235
	4	4	293
$S^{-1}_1(p_0)$	1	19	279
	2	134	109
	3	40	174
$S^0_1(p_0)$	0	12	154
	1	16	301
	2	61	182

Because of the very irregular geographical distribution of the diurnal surface pressure oscillation the expression (7) does, of course, only give a very broad picture of the diurnal pressure oscillation. It is of some interest to inquire how this large-scale pattern is modified by the additional component waves given in Table 2 and by the higher modes which have not been computed.

To obtain a quantitative idea of the difference some numbers have been computed which may be called the "errors" of expression (7) and of a more complete expression involving all those terms of Table 2 whose amplitudes are 40 μb or larger. The latter expression depends, of course, not only on colatitude, but also on longitude. Let p and q be the sine and cosine factors explained in (1) which are read off from the 336 grid points in Fig. 1 and 2 and which were used for the harmonic analysis along latitude circles. Let further p^* and q^* be the same quantities, but computed from (7) for the same grid points. Finally, let $\bar{p}$ and $\bar{q}$ be these same coefficients, but computed from the more complete expressions for the

diurnal pressure wave when all terms indicated in Table 2 with amplitudes $\geqq 40\ \mu b$ are used. The following two quantities have been computed

$$\sum_{336}\left[\frac{(p-p^*)^2+(q-q^*)^2}{n}\right]^{1/2}=248\ \mu\text{b}$$

and

$$\sum_{336}\left[\frac{(p-p)^2+(q-q)^2}{n}\right]^{1/2}=209\ \mu\text{b}.$$

Both figures show first of all that the theoretical expressions obtained by harmonic analyses do not reproduce the details of the geographical distribution very well. The shorter waves with higher wave numbers not

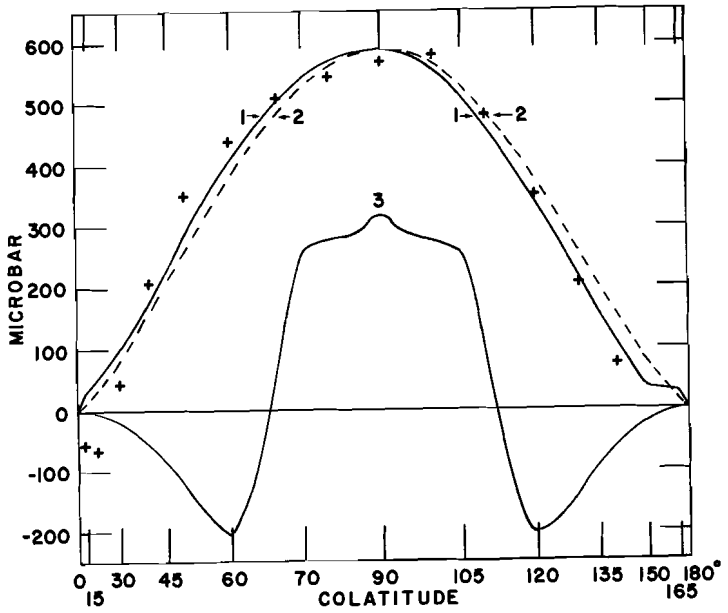

Fig. 4. The amplitude of the main part of the diurnal pressure oscillation as a function of the colatitude. Crosses: Amplitudes determined from the data. Curve 1: Distribution given by the first three associated Legendre functions of order 1. Curve 2: Distribution given by $\sin^3\vartheta$. Curve 3: Distribution given by the first three symmetrical Hough functions

considered in the calculations leading to Table 2 which appear because of the geographical irregularities and which may be regarded as "noise" superimposed on the planetary diurnal pressure oscillation, contribute an appreciable fraction of the total energy. Our aim here is to obtain an expression for the main, planetary part of the diurnal pressure wave, rather than a formula giving the fine details of its geographical distribution. For this purpose it is important that the more complicated expression involving 8 terms of Table 2 does not give a substantially smaller "error" than the simple expression (7). The latter, or even (8), may therefore be regarded as representing the main part of the planetary diurnal pressure wave.

IV. Discussion

Since the diurnal pressure wave is excited by the diurnal temperature wave, the two waves must be compared with each other. But for the diurnal temperature wave, only the largest component, $S_1^1\ (T_0)$, that is the wave migrating with the same speed as the sun, has been analyzed. One of these analyses (HAURWITZ [*10*]) is partly based on empirical data. The theoretical analysis by KERTZ [*13*] takes into account the effects of turbulent mass exchange and of radiation while that by SIEBERT considers only the temperature changes due to absorption of solar radiation. The coefficients given in these three papers are reproduced in Table 3. Since the analysis of the empirical data is based on annual mean values only the values for the equinoxes computed by KERTZ and SIEBERT [*22*] are given here.

Only the first three harmonic terms are shown. Since the second terms are quite large unless radiation only is considered, and since P_2^1 is asymmetrical with respect to the equator the temperature wave is much less

Table 3. *Harmonic Coefficients of the Diurnal Surface Temperature Wave*

		HAURWITZ		KERTZ		SIEBERT	
Wave Type	$\lvert s\rvert+i$	Ampl.	Phase const.	Ampl.	Phase const.	Ampl.	Phase const.
$S_1^1\ (T_0)$	1	1.007° C	232°	0.748° C	225°	0.158° C	180°
	2	0.647	232	0.439	225	—	—
	3	0.502	238	0.083	225	0.020	0

symmetrical with respect to the equator than the pressure wave. As shown by LAPLACE (see for instance LAMB [*15*]) no changes in the elevation of the free surface of an ocean of uniform depth covering the whole earth will occur if the generating force is of the form $P_2^1\ (\vartheta)$. We may therefore surmise that the corresponding term in the diurnal temperature oscillation will not cause an appreciable pressure oscillation of this form.

For a comparison between the forcing function, that is the temperature wave and the resulting pressure oscillation, one should use the temperature oscillation throughout the whole atmosphere rather than that at the earth's surface. But only the latter has been analyzed and must therefore be used here. It can be expected that the distribution of $S_1\ (T)$ in the higher atmosphere is less influenced by the small-scale geographic features than at the ground. Hence, the sum of the lowest-degree Legendre functions should give a better approximation to the diurnal temperature wave for the whole atmosphere than to $S_1\ (T_0)$.

The associated Legendre functions used here to describe the latitudinal variations of the diurnal pressure oscillation are not suitable for the com-

parison between forcing function and resulting oscillation. The dependence of the oscillation on the latitude is described by Laplace's tidal equation. The solutions of this equation are given by "Hough" functions, named after HOUGH [11] who studied this equation extensively. These functions are most easily expressed in series of associated Legendre functions because for many of the important oscillations the difference between the Hough functions and the corresponding associated Legendre function is quite insignificant (as long as the depth of the equivalent ocean is not too small).

However, for the diurnal oscillations of the atmosphere the equivalent depths are small so that the series of associated Legendre functions expressing the Hough functions converge very slowly. The three largest equivalent depths belonging to diurnal oscillations symmetrical to the equator, h_1^1, h_3^1, h_5^1 and the corresponding Hough functions have been computed. In these computations the small difference between the length of the solar day and of the sidereal day can be neglected. The relevant parameter in Laplace's tidal equation is actually $N_k^1 = g\, h_k^1/4\, \omega^2\, a^2$ where g is the acceleration of gravity at the surface, ω the angular velocity of rotation, a is the radius of the rotating sphere. In the case of the earth

$$N_k^1 = 11.35 \cdot 10^{-6}\, h_k^1$$

where h_k^1 is expressed in meters. The values for the three highest symmetrical modes are shown in Table 4.

Table 4. *Equivalent Depths for the Diurnal Oscillation*

k	1	3	5
N_k^1	$0.7930 \cdot 10^{-2}$	$0.1380 \cdot 10^{-2}$	$0.0555 \cdot 10^{-2}$
h_k^1	699 m[1]	122 m	48.9 m

[1] W. KERTZ found earlier 634 m for this value (see SIEBERT [22]), but he has informed that the larger value given here is correct.

The Hough functions are given in the form

$$\Theta_k^1 = \sum_{i=1}^{\infty} d_{ki}^1\, P_i^1(\vartheta) \tag{9}$$

where $P_i^1(\vartheta)$ is the seminormalized associated Legendre function for which

$$\int_{-\frac{\pi}{2}}^{\frac{\pi}{2}} P_i^m(\vartheta)^2 \sin\vartheta\, d\vartheta = \frac{4}{2i+1} \quad (m \geq 1).$$

The coefficients d_{ki}^1 are given in Table 5. The arbitrary constant is chosen so that the coefficient $d_{ii}^1 = 1$. The convergence of the series, especially that for Θ_5^1 is poor, even if it is remembered that for the seminormalized Legendre functions the quadratic mean value decreases with increasing i.

Table 5.
Coefficients of the Symmetrical Hough Functions for the Diurnal Oscillation[1]

	$\Theta_k^1 = \sum_i d_{ki}^1\, P_i^1(\vartheta)$		
i/k	1	3	5
1	1	— .3073	+ .827
3	— 3.4422	1	— 2.671
5	+ 4.1748	— .4733	1
7	— 2.6256	— 2.2338	+ 6.508
9	+ 1.0200	+ 5.3936	— 13.140
11	— .2694	— 6.6915	+ 9.084
13	+ .0515	+ 5.7104	+ 7.143
15	— .0074	— 3.6884	— 26.676
17	+ .0008	+ 1.8931	+ 38.806
19	— .00008	— .7958	— 39.324
21		+ .2798	+ 31.333
23		— .0834	— 20.652
25		+ .0206	+ 11.565
27			— 5.536
29			+ 2.097

[1] More complete and accurate values of these coefficients have been computed by Mr. THOMAS FLATTERY of the Department of the Geophysical Sciences of the University of Chicago.

Table 6. *Symmetric Hough Functions of Order 1*

	Θ_1^1	Θ_3^1	Θ_5^1	
0°	0	0	0	180°
5	— .00190	.00034	.00599	175
10	— .00479	— .00023	— .00518	170
15	— .01012	— .00000	.00323	165
20	— .02027	.00006	— .00359	160
25	— .03918	— .00001	.00067	155
30	— .07267	.00125	— .00093	150
35	— .12797	.00512	— .00231	145
40	— .21133	.01999	.00003	140
45	— .32244	.06423	— .01966	135
50	— .44609	.16339	— .06704	130
55	— .54414	.31347	— .22169	125
60	— .55531	.39163	— .33159	120
65	— .41153	.14727	.02675	115
70	— .07264	— .50711	.82616	110
75	.43355	— 1.06616	.49917	105
80	.99329	— .71546	— .88817	100
85	1.43554	.45771	— .25076	95
90	1.60405	1.13620	1.00270	90

For the subsequent numerical calculations it is more convenient to choose the arbitrary constant so that the largest coefficient in the series becomes unity. Accordingly Θ_1^1 has been divided by $d_{1,5}^1$, Θ_3^1 by the absolute value of $d_{3,11}^1$, Θ_5^1 by the absolute value of $d_{5,19}^1$. The numerical values of Θ_k^1 reduced in this manner are reproduced in Table 6 for intervals of 5° colatitude and are plotted in Fig. 5. With the new choice of the arbitrary constants all three Hough functions are similar in magnitude. Both Table 6 and Fig. 5 show that the functions are large only in a belt of 60°

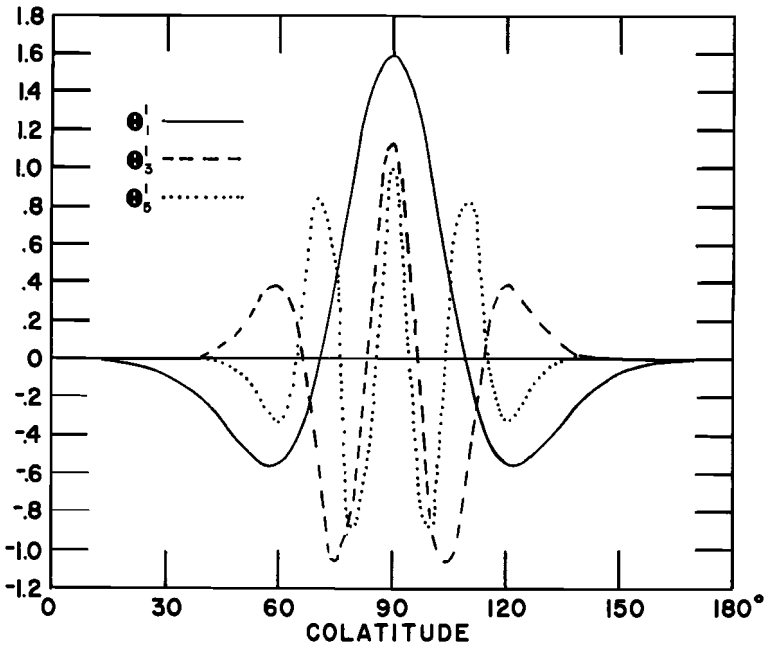

Fig. 5. The first three symmetrical Hough functions. (The arbitrary constant has been chosen so that the largest factor in the series of associated Legendre functions is one)

width centered at the equator and that the higher modes oscillate strongly. As will be seen and as might be expected this behavior makes them not very suitable for a representation of the observed data. The values of Θ_k^1 for the higher modes are given to a greater degree of accuracy than warranted by the computed series (Table 5) in order to facilitate corrections by extending these series. The coefficients for the development of $S_1^1\,(p_0)$ in terms of the first three symmetrical Hough functions have been determined by the method of least squares directly from the harmonic coefficients c and s, explained in the scheme at the beginning of Section 3. As in the computation of the coefficients f and g in (5) a weighting factor $\sin\vartheta_r$ has been used to allow for the reduction in area of the latitude belts

polewards. But as in Section 3, despite the orthogonality of the Hough functions, the earlier coefficients in the series of Hough functions would have to be recomputed if more terms are taken since the data available here extend only to 140° colatitude.

The terms in the series of Hough functions representing $S_1^1\,(p_0)$ may be written in either of the two forms

$$[u_k \cos(t+\lambda) + v_k \sin(t+\lambda)]\,\Theta_k^1(\vartheta) = W_k \sin(t+\lambda+\varphi_k)\,\Theta_k^1(\vartheta). \quad (10)$$

The constants u_k, v_k, W_k, and φ_k are shown in Table 7. The angle φ_k for all three terms considered here is very similar either to 20.4°, its value for the leading term, of to 180° + 20.4°. One may therefore write.

$$\begin{aligned} S_1^1\,(p_0) = \{&[248\ \theta_1^1 - 117\ \theta_3^1 + 56\ \theta_5^1]\sin(t+\lambda+20.4°)\,. \\ &+ [7\ \theta_3^1 - 2\,\theta_5^1]\cos(t+\lambda+20.4°)\}\,\mu b \end{aligned} \quad (11)$$

where the cosine term can clearly be omitted. The phase angle is here 8° larger than in the previous expressions for $S_1^1\,(p_0)$, (7) and (8), so that the maximum would occur only about half an hour earlier than according to (7) or (8).

The latitude distribution of the amplitude of $S_1^1\,(p_0)$ according to (11) is shown in Fig. 4 as curve 3. It gives only a poor approximation. Even in the equatorial zone the amplitudes are only about half of those determined by harmonic analysis along latitude circles. Nevertheless, an attempt will be made to compare the coefficient for $S_1^1\,(p_0)$ given in Table 7

Table 7. *Representation of $S_1^1\,(p_0)$ and $S_1^1\,(T_0)$ by Hough Functions*

k	u_k	v_k	W_k	φ_k	f_k HAURWITZ	f_k SIEBERT
1	86 μb	232 μb	248 μb	20.4°	0.098° C	0.064° C
3	— 34	— 112	117	196.9	— 0.047	— 0.027
5	18	53	56	18.7	0.037	0.015

with theoretical estimates. For this purpose the temperature wave $S_1^1\,(T)$ has to be known as a series of Hough functions. Since we are here concerned only with the part of the diurnal pressure oscillation symmetrical to the equator, only the symmetrical terms of the temperature series are considered, that is the terms with $P_1^1\,(\vartheta)$ and $P_3^1\,(\vartheta)$, given in Table 3. If this part of the temperature series is expressed by the first three symmetrical Hough functions the coefficients f_k in Table 7 are obtained in the same manner as the coefficients for the pressure series, after the temperature amplitudes for each tenth degree of colatitude have been computed from the data in Table 3. The first set of f_k has been determined from the semi-empirical values of Haurwitz, the other from Siebert's values. Because of the form of the functions θ_k^1 the difference between the two sets of f_k is much smaller than might be expected from Table 3.

To obtain an estimate of the theoretical response of the atmosphere to the modes of the temperature oscillation given in Table 7 some formulae given by SIEBERT [22] can be used. Although these formulae are derived under various simplifying assumptions they will at least give approximately the response of the atmosphere to the temperature oscillation. It is assumed here that the atmosphere is isothermal because the somewhat more realistic temperature distribution considered by SIEBERT with a temperature gradient decreasing to zero does not give substantially different results. The following notations are used:

h_n equivalent depth of vibration of mode n

$\varkappa = 2/7$

H scale height, assumed constant and equal to 8.2 km

$b_n = -[(4\,\varkappa\,H/h_n) - 1]^{1/2}$

$p_0 = 1000$ mb, $T_0 = 280$ K, mean surface pressure and temperature

$\delta\,p_n\,(0)$, $\tau_n\,(0)$ change of surface pressure and temperature due to the nth mode

K coefficient of turbulent mass exchange, assumed equal to 10^4 cm^2/sec

$k = 1/3$, coefficient to allow for absorption of solar radiation

σ = frequency of oscillation

Then, if the daily temperature wave is due to direct absorption

$$\delta\,p_n\,(0) = -\frac{p_0\,H\,h_n\,(1 + 2\,k - b_n)\,\tau_n\,(0)}{T_0\,[2\,H - h_n\,(1 + b_n)]\,[(1 + k)\,k\,h_n + \varkappa\,H]}\,. \qquad (12)$$

If the daily temperature wave is largely due to heat transport upward one has to put in this formula

$$k = H\left(\frac{\sigma}{K}\right)^{1/2} e^{i\frac{\pi}{4}} \qquad (13)$$

as shown by SIEBERT. If only eddy transfer is considered one obtains for the lowest mode θ_1^1 a pressure variation which is about 50 times too small with the larger value of f_1. This result merely confirms the conclusion of SIEBERT [22] and others that the solar oscillations of the atmosphere must largely be due not to the heat wave propagated upward by eddy conductivity, but due to direct absorption of solar radiation.

M. SIEBERT has suggested to me that when determining the effect of the diurnal heat wave caused by solar radiation alone on the diurnal pressure wave the values f_k computed from the results of his theoretical studies should be chosen because those obtained from my empirical investigation contain the effects of turbulent transfer and radiation which both affect the temperature in the lowest layer. In the following the values of f_k determined from SIEBERT's computations will therefore be used. With eq. (12) it is found that corresponding to the W_k of Table 7

$$|\,\delta\,p_1\,(0)\,| = 140\ \mu\text{b}\ (220\ \mu\text{b})$$
$$|\,\delta\,p_3\,(0)\,| = 25\ \mu\text{b}\ (44\ \mu\text{b})$$
$$|\,\delta\,p_5\,(0)\,| = 15\ \mu\text{b}\ (21\ \mu\text{b}).$$

In parentheses the amplitudes computed from (12) with the other set of f_k values are shown merely for comparison. In contrast to the semidiurnal oscillation the diurnal pressure oscillation produced by the corresponding temperature wave is very small, although it is ten times larger than the value found by BUTLER and SMALL [1] for $\delta\,p_1\,(0)$ as the effect of the diurnal temperature wave in the ozone layer alone, without the effect of absorption of solar radiation by water vapor in the lower layers.

Before the significance of the results for the theory of the thermal excitation of the atmospheric tides is discussed in the next Section the phase constant may be briefly considered. According to SIEBERT the phase constant of the leading term in the series for the temperature wave is 180° (see Table 3 above). The minus sign in (12) shows that the phase constant of the corresponding pressure oscillation mode should be zero giving a pressure maximum at 6 a. m. Since phase angle φ_1 derived from the data (see Table 7 or [11]) is 20.4° the pressure maximum occurs actually 1.4 hours earlier. The difference may be partly due to the inaccuray of the data. It may in part also be caused by the highly simplified calculations of SIEBERT which consider only the effect of absorption, but not of emission of radiation. Because of the latter the temperature will no longer have its maximum at 6 p. m. (phase angle 180°) when the solar energy becomes zero, but earlier namely when the energy radiated by the atmosphere equals the absorbed energy. Thus, the phase constant of the temperature wave will be larger than 180°, and consequently that of the pressure wave larger than zero.

V. Conclusion

One of the main problems of atmospheric tidal theory is to explain the small size of $S_1\,(p_0)$ as compared to $S_2\,(p_0)$. In the absence of large resonance magnification, thermal rather than gravitational excitation must account for both oscillations. But the diurnal temperature wave is about 2.5 stronger than the semidiurnal component. Our spherical harmonic analysis has shown that the predominant component of $S_1^1\,(p_0)$ amounts in fact to half of $S_2\,(p_0)$ so that the difference in size of the two oscillations is not as large as is often believed. The amplitude factor of θ_1^1 in (11), the largest term in the expression for $S_1^1\,(p_0)$ in a series of Hough functions, is about 70 percent larger than the theoretical estimate based on (12), as shown in the preceding Section. Because of the inadequacy of the empirial data for $S_1^1\,(p_0)$ this must be considered quite fair agreement between observation and the theory of thermal excitation. The temperature amplitude for the mode θ_1^1 is very small, according to Table 7, because the form of the function $\theta_1^1\,(\vartheta)$ with its small equivalent depth differs greatly from the latitudinal distribution of the diurnal temperature wave. It must be partly due to this fact that the corresponding mode of the diurnal pressure wave is also small. For the semidiurnal solar tide with its eleven times larger equivalent depth, the relevant Hough function $\theta_2^2\,(\vartheta)$ is very similar to the corresponding associated Legendre function $P_2^2\,(\vartheta)$ whose factor is 0.32° C (HAURWITZ [10]). Hence, the amplitude

of the exciting semidiurnal temperature wave is in fact considerably larger than that for θ_1^1. In other words, the geographical distribution of the semidiurnal temperature wave is such that it is much more effective in producing a corresponding pressure oscillation than the diurnal temperature wave. This had already been surmised by SIEBERT [22] before the form of $\theta_1^1(\vartheta)$ was known, when he suggested that the diurnal pressure oscillation is suppressed in the atmosphere.

Further, because of the small equivalent depth of the mode θ_1^1 the corresponding pressure oscillation would be smaller than the semidiurnal oscillation even if the two exciting temperature waves were equal in magnitude. One finds from (12), since the equivalent depth of the semidiurnal oscillation $h_2 = 7.85$ km, that $\delta p_2(0)$ should be about three times larger than $\delta p_1(0)$ if the two temperature amplitudes were equal. Without carrying this discussion any further, it is thus clear that there is no difficulty in explaining the smaller magnitude of $S_1(p_0)$ than of $S_2(p_0)$, and that thermal excitation provides not only a satisfactory explanation of the observed magnitude of the semidiurnal pressure oscillation, but also of the smallness of the diurnal oscillation.

Acknowledgement

I am indebted to Professor R. SAWADA and to Dr. M. SIEBERT for discussion of the problems considered here and Mrs. A. D. COWLEY for performing and programming the required calculations.

References

1. BUTLER, S. T., and K. A. SMALL: The Excitation of Atmospheric Oscillations. Proc. Roy. Soc. (London) A **274**, 91—121 (1963).
2. CHAPMAN, S.: Lunar Atmospheric Tide over Canada, 1897—1932. Quart. J. Roy. Met. Soc. **61**, 359—366 (1935).
3. CHAPMAN, S.: The Lunar Atmospheric Tide at Accra, Gold Coast. Quart. J. Roy. Met. Soc. **64**, 523—524 (1938).
4. FROST, R.: Pressure Variation over Malaya and the Resonance Theory. Air Ministry, Scient. Pap. 4, 13 pp. (1960).
5. HANN, J.: Untersuchungen über die tägliche Oscillation des Barometers. Denkschr. Akad. Wiss., Wien, Math.-Nat. Kl. **55**, 49—121 (1889).
6. HANN, J.: Weitere Untersuchungen über die tägliche Oscillation des Barometers. Denkschr. Akad. Wiss., Wien, Math.-Nat. Kl. **59**, 297—356 (1892).
7. HANN, J.: Untersuchungen über die tägliche Oscillation des Barometers. III. Denkschr. Akad. Wiss., Wien, Math.-Nat. Kl. **95**, 1—64 (1917).
8. HANN, J.: Die jährliche Periode der halbtägigen Luftdruckschwankung. Sitz. Ber. Akad. Wiss., Wien, Math.-Nat. Kl. (II a) **127**, 263—365 (1918).
9. HAURWITZ, B.: The Geographical Distribution of the Solar Semidiurnal Pressure Oscillation. Meteorol. Papers, Vol. 2, 5. 36 pp. New York, 1956.
10. HAURWITZ, B.: Die tägliche Periode der Lufttemperatur in Bodennähe und ihre geographische Verteilung. Arch. Met. Geoph. Biokl. A **12**, 426—434 (1962).
11. HOUGH, S. S.: On the Application of Harmonic Analysis to the Dynamical Theory of Tides. Phil. Trans. Roy. Soc. (London) A **189**, 201—257, A **191**, 139—185 (1898).

12. KELVIN, Lord (W. THOMSON): On the Thermodynamic Acceleration of the Earth's Rotation. Proc. Roy. Soc. Edinburgh **11**, 396—405 (1882).
13. KERTZ, W.: Atmosphärische Gezeiten. In: Handbuch der Physik, Vol. 48, pp. 928—981. Berlin, 1957.
14. KERTZ, W.: Partialwellen in den halb- und vierteltäglichen gezeitenartigen Schwingungen der Atmosphäre. Arch. Met. Geoph. Biokl. A **11**, 48—63 (1959).
15. LAMB, H.: Hydrodynamics, 6th ed., 738 pp. New York. See pp. 341—342.
16. PEKERIS, C. L.: Atmospheric Oscillations. Proc. Roy. Soc. (London) A **158**, 650—671 (1937).
17. ROSENTHAL, S. L., and W. A. BAUM: Diurnal Variation of Surface Pressure over the North Atlantic Ocean. Mo. Weather Rev. **84**, 379—387 (1956).
18. SCHOU, G.: Mittel und Extreme des Luftdruckes in Norwegen. Geophys. Publ. **14**, 2 (1939).
19. SELLICK, N. P.: Note on the Diurnal and Semidiurnal Pressure Variation in Rhodesia. Quart. J. Roy. Met. Soc. **74**, 78—81 (1948).
20. SEN, H. K., and M. L. WHITE: Thermal and Gravitational Excitation of Atmospheric Oscillations. J. Geophys. Res. **60**, 483—495 (1955).
21. SIEBERT, M.: Zur Theorie der thermischen Erregung gezeitenartiger Schwingungen der Erdatmosphäre. Naturwissenschaften **41**, 446 (1954).
22. SIEBERT, M.: Atmospheric Tides. In: "Advances in Geophysics", Vol. 7, pp. 105—187. New York, London, 1961.
23. SOLBERG, H.: Über die freien Schwingungen einer rotierenden Flüssigkeitsschicht auf der rotierenden Erde I. Astrophysica Norwegica **1**, 7, 237—340 (1936).

Author's address: Dr. BERNHARD HAURWITZ, National Center for Atmospheric Research, Boulder, Colorado 80301, U.S.A.

Printed in Austria

Reprinted from Science, June 19, 1964, Vol. 144, No. 3625, pages 1415-1422

Atmospheric Tides

These oscillations are caused by the gravitational pull of sun and moon and by the sun's thermal effects.

B. Haurwitz

The term *atmospheric tides* refers not only to the atmospheric oscillations produced by the gravitational forces of the moon and the sun but also to the oscillations due to the sun's thermal effects on the earth's atmosphere. This dual meaning is theoretically appropriate, since both gravitational forces and thermal effects induce oscillations which are gravity waves. Also, it is necessary for practical reasons to consider these two effects together, since one cannot separate them in the case of the oscillation of 12-hour period which appears both in the sun's tide-producing gravitational attraction and in the thermal influence of the sun on the atmosphere.

Barograph traces at the earth's surface show that in tropical regions the pressure has two maxima and two minima per day, the maxima occurring at about 10 a.m. and 10 p.m. local mean time, the minima occurring, respectively, 6 hours later. The amplitude of these oscillations is about 1 millibar (*1*). Figure 1 shows the hourly values for barometric pressure for a week at Balboa, Panama. At higher latitudes the nonperiodic pressure changes due to the passage of weather systems are very much larger than they are in the tropics and mask, in general, the 12-hourly oscillation. To find this oscillation a statistical investigation is required, based on a sufficiently long record to permit elimination of the irregular pressure changes.

Figure 1 shows clearly that the pressure oscillation has a period of half a solar day (12 hours), rather than of half a lunar day (12 hours 26 minutes). On the other hand, the gravitational tidal force of the moon is 2.2 times that of the sun. Therefore, one of the main problems of the theory of atmospheric tides is the need to explain why the solar tide is so much stronger than the lunar tide in the atmosphere. Laplace suggested early in the 19th century that the solar tide might be caused by the thermal rather than the gravitational action of the sun on the atmosphere. The daily temperature curve is not a pure sine wave; it contains, in addition to the 24-hourly oscillation, oscillations of higher frequencies—in particular, an oscillation of 12-hour period, discussed later. The amplitude of the 12-hourly temperature wave is smaller than that of the 24-hourly temperature wave, hence it becomes necessary to explain why the amplitude of the 12-hourly pressure wave is greater than that of the 24-hourly pressure wave. Kelvin (*2*) conjectured that the atmosphere may have a free oscillation of period of about 12 hours, and that the 12-hourly oscillation (but not the 24-hourly oscillation) is thus magnified through resonance. This suggestion is now generally referred to as the "resonance theory" of the semidiurnal pressure oscillation. Later I describe this theory and its development and modification in detail, but first it is necessary to discuss the observational information available on the atmospheric tides. This discussion is confined largely to the tidal variation of meteorological parameters, especially of pressure and wind. Only occasionally do I refer to the tidal variations of geomagnetic and ionospheric parameters.

For conciseness and clarity the notations L_n and S_n are used in the discussion of lunar and solar variations of geophysical parameters. The subscript n indicates that the period referred to is the nth part of the (lunar or solar) day. Where necessary, the parameter under discussion is shown in parenthesis. For instance, $S_2(p_0)$ denotes the solar semidiurnal oscillation of the sea-level barometric pressure p_0.

The Lunar Atmospheric Tide

Although the lunar atmospheric tide L_2 is about 15 times smaller than the solar atmospheric tide S_2, it can nevertheless be found, by means of statistical methods, from long series of data (*3*). The results of a determination of the lunar tide (and, with appropriate changes, of the solar tide) are customarily expressed in the form of a sine wave

$$L_n = A_n \sin (15\, n\tau + \alpha_n) \qquad (1)$$

where n is the fraction of the day, τ is the local lunar mean time (in hours), A_n is the amplitude, and α_n is the phase constant of the oscillation. In the case of the lunar tide only the semidiurnal oscillation ($n = 2$) has been found so far in meteorological variables, whereas in the case of the solar tide, S_1, S_2, S_3, and S_4 have been determined. From the phase angle α_n the time of the maximum can readily be obtained, since the argument of the sine must then be 90 degrees. For example, the annual mean value for the

The author is professor of geophysics in the department of astrophysics and atmospheric physics of the University of Colorado, Boulder, and is also on the staff of the National Center for Atmospheric Research, Boulder.

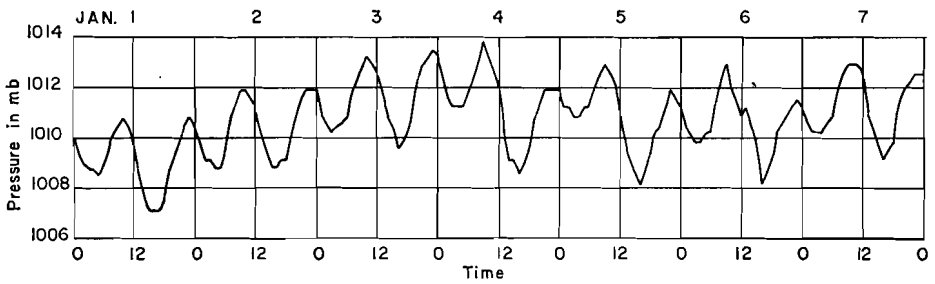

Fig. 1. Surface barometric pressure at Balboa, Panama, from 1 to 7 January 1952.

lunar tide in the barometric pressure p_o at sea level at Balboa, Panama, as determined from data for 17.5 years, is

$$L_2(p_o) = 58.3 \cdot 10^{-3} \text{ mb} \sin (30_T + 77.0°), \quad (2)$$

hence the maximum occurs about half an hour after the moon passes the local meridian. This variation due to the lunar tide is illustrated in Fig. 2 (left). The two numbers characterizing the oscillation are the amplitude and the phase angle. These, and therefore the whole oscillation, can be represented more concisely in a polar diagram, where the distance from the center 0 represents the amplitude, and where the phase constant is plotted so that the time of the maximum can be read off the diagram directly. Figure 2 (right) is a polar diagram for $L_2(p_o)$ at Balboa, the annual mean being represented by point A. (Because all plotted points lie in one quadrant, only this quadrant is shown.) The direction of the line $0A$ shows the phase constant, in degrees (outer scale at the circumference) and as the time of the maximum (inner scale). Since, for a 12-hourly oscillation, this type of figure is similar to a clock face, it is called a "harmonic *dial*."

Because long series of data are required for finding the variation in atmospheric pressure caused by the lunar tide, this variation has so far been determined at only about 70 stations. The determinations have been mainly the work of S. Chapman (*4*). Figure 3, which is largely based on Chapman's results, shows the global distribution of the amplitude of this tide. The amplitude decreases from the equator poleward, as would be expected, since the lunar tidal force decreases toward the poles. In general, the high tide occurs about ½ to 1 hour after passage of the moon through the local meridian. But there are, despite the regular distribution of the lunar tidal force, some very striking irregularities in the distribution of the lunar atmospheric tide. One of these is the smallness of the lunar tide on the Pacific coast of North America, presumably due to the obstructing effects of the mountains on the westward progression of the tide. Another irregularity is the asymmetry of the amplitude with respect to the earth's equator; there are large amplitudes over the eastern part of Africa south of the equator and over the western part of Indonesia. No explanation of this phenomenon has yet been proposed.

If we group the months into three "seasons," designated *D* (November, *D*ecember, January, February), *E* (for *E*quinoctial) (March, April, September, October), and *J* (May, June, July, August), we obtain for Balboa (Fig. 2, right) the three points *J*, *E*, and *D*, which are connected by straight lines indicating a pronounced seasonal variation. The circles around these points are probable-error circles (*3*) of $L_2(p_o)$ for each season. A determination of such oscillations cannot be considered satisfactory if the radius of the probable-error circle is more than one-third the amplitude. The determinations of Fig. 2 (right) are clearly satisfactory. The seasonal variation for Balboa is fairly typical: largest amplitudes around the June solstice, smallest amplitudes around the December solstice. Contrary to many meterological variables with a seasonal period, the maxima and minima for L_2 occur at the same time of the year, rather than with opposite phases, in the Northern and Southern hemispheres. Since the lunar tidal force has no seasonal variation, the cause of the seasonal variation of the lunar atmospheric tide must be sought in the varying response of the atmosphere to this force. But no satisfactory explanation has as yet been offered. An understanding of the apparently anomalous responses of the

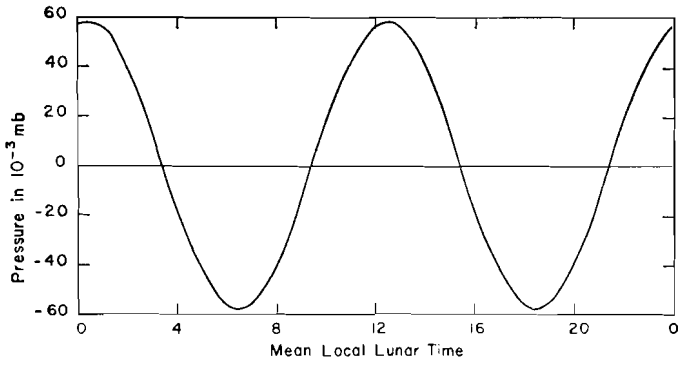

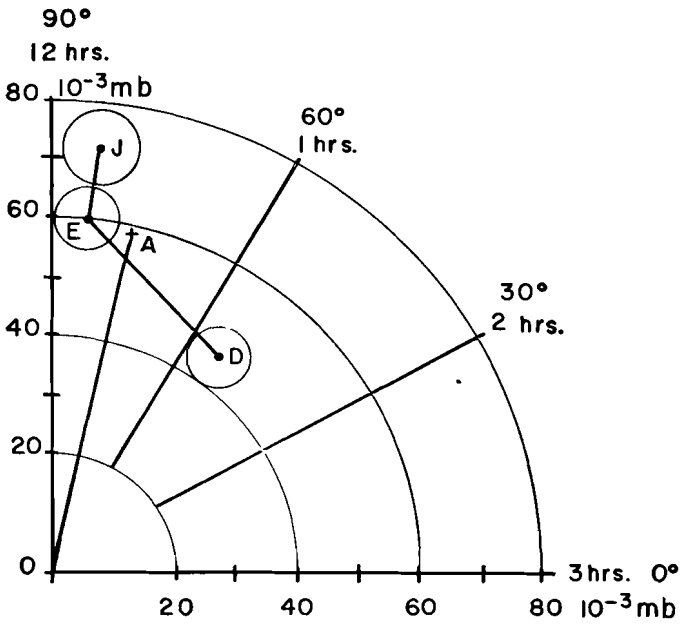

Fig. 2. The lunar tide in the earth's atmosphere at Balboa, Panama, as determined from data accumulated over 17.5 years. (Left above) Variation of pressure at the earth's surface due to the lunar tide. (Right) Harmonic dial showing seasonal variation: (*J*) summer months; (*D*) winter months; (*E*) equinoctial months; (*A*) annual mean.

analysis of all the available data, the following approximate expression is obtained

$$S_1(p_s) = 0.59 \text{ mb } \cos^3 \phi \sin (t + 12°) \quad (4)$$

where the meaning of the symbols is the same as in Eq. 3. The magnitude of this oscillation is thus about half that of the semidiurnal oscillation, and its maximum occurs shortly after 5 a.m. local mean time. S_1 and S_2 undergo seasonal variation. Even for S_2 these variations differ greatly at different stations.

The higher harmonics, S_3 and S_4, as well as the standing component of S_2, can be produced only by the thermal action of the sun, since the sun's tide-producing gravitational force does not contain any corresponding terms. S_3 is considerably smaller than S_1 and S_2. Its maximum amplitude of about 0.2 mb occurs at about 30° north and 30° south latitude. Despite its smallness it is very regularly distributed over the globe. An interesting feature of S_3 is its pronounced seasonal variation with phase reversals between January and July and minimum amplitude at about the time of the equinoxes; this corresponds to the seasonal variation of the 8-hourly temperature variation. S_4 is even smaller than S_3, but it also has a fairly regular distribution over the earth, and this makes it interesting from the standpoint of theory.

Atmospheric Tides at Higher Levels

The tidal oscillations near the earth's surface are very small as compared to the mean for low levels of the atmosphere; the oscillations are very much larger at high levels. The first, indirect, evidence of the importance of the atmospheric tides at great heights was furnished by the daily variations (according to both solar and lunar time) of the geomagnetic parameters. An explanation of these variations is given by the "dynamo" theory. According to this theory a current is induced in the ionized layers of the high atmosphere when they are moving in the geomagnetic field because of the atmospheric tides. At the surface, the effects of this current are observed as the daily variations of the geomagnetic parameters.

Direct evidence of the tides in the high atmosphere has been obtained only fairly recently, through observation, by means of radio techniques, of the drift of meteor trails. When a meteor penetrates the atmosphere down to a level of about 80 to 100 kilometers it produces an ionized trail during its disintegration as it collides with the air molecules. This trail drifts along with the air. Radio signals are reflected from these meteor trails, and the radial-drift velocity, with respect to the observer, can be found by means of Doppler techniques. The wind velocity can be determined from these radial velocities, because in a reasonably short time a sufficient number of radio meteor echoes from different directions can be observed to compute this velocity.

Such data have, so far, been obtained mainly at two stations—at Jodrell Bank, near Manchester, England, and at Adelaide, Australia. The Jodrell

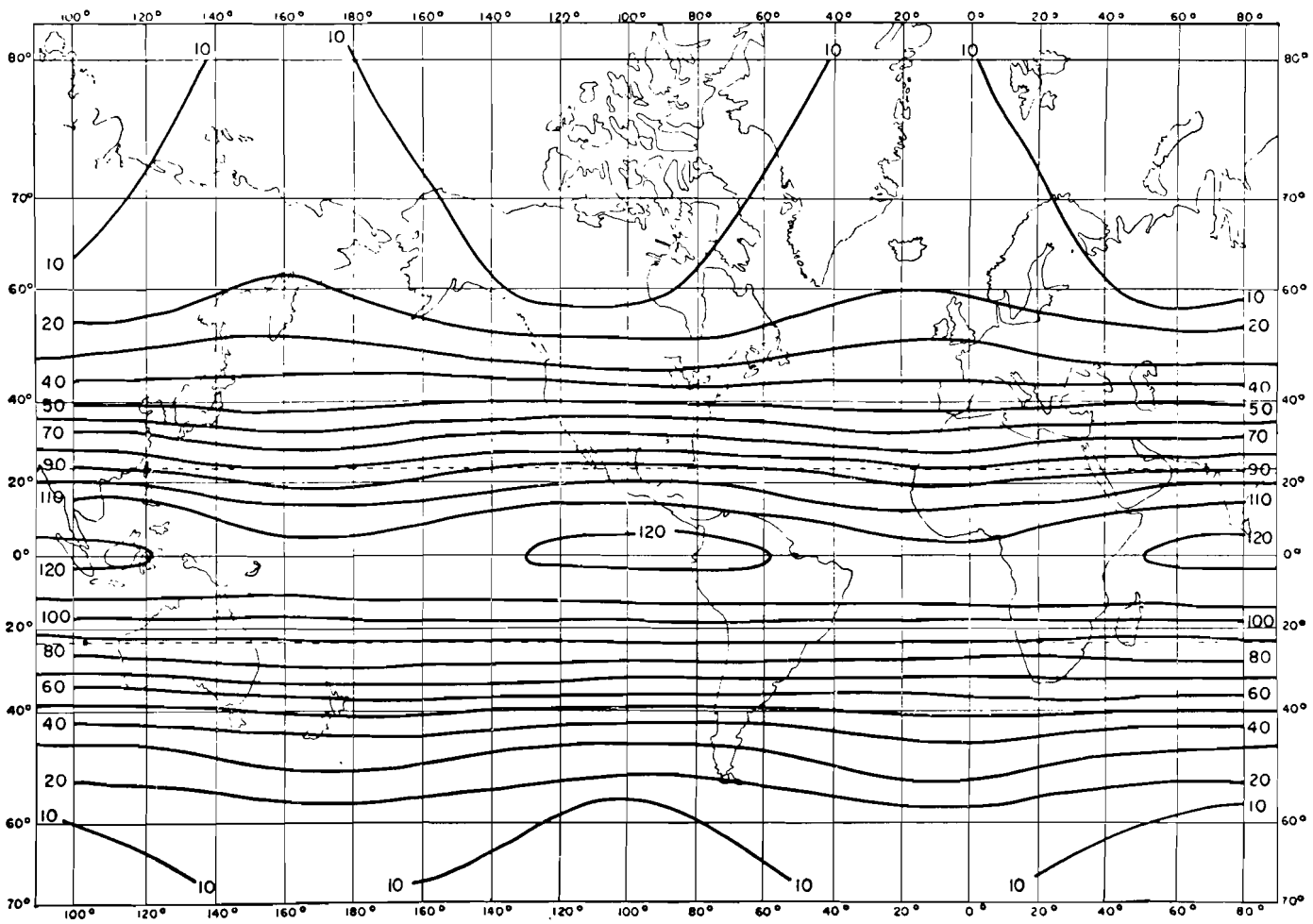

Fig. 4. Lines of equal amplitude for the semidiurnal solar tide as manifested in atmospheric pressure at the earth's surface (see *16*). The amplitude is given in units of 10^{-2} millibar.

Bank data were obtained by Greenhow and Neufeld; the Adelaide data, by Elford (*6*). The data show that the amplitudes of the periodic variations of the wind components, both S_1 and S_2, are similar in magnitude to the daily mean wind, and that in both cases the amplitudes are about 100 times greater in the high atmosphere than at the ground. The behavior of the periodic part of the wind is illustrated in Fig. 6. Here the speed and direction of the wind are plotted as hodographs, which show the end point of the periodic wind vector $S_1 + S_2$ for the D months. The numbers from 0 to 22 adjoining the marked points on the hodograph curve give every second hour in local mean time. Thus, in Fig. 6 (left) for Jodrell Bank, the wind at local midnight (0 hours) blows nearly toward south (a "north wind" in meteorological and everyday terminology) with a speed of about 16 meters per second. The wind vector turns clockwise and describes two complete rotations during 24 hours, demonstrating the presence of the semidiurnal oscillation. Because the 24-hourly oscillation is superposed, the two circuits do not coincide. At Adelaide (Fig. 6, right) the wind vector turns counterclockwise, as it should in the Southern Hemisphere. The hodograph curve does not show two complete loops, because here S_1 has a larger amplitude than S_2. It is impossible to say, on the basis of presently available data, whether in general S_2 or S_1 is larger at these high altitudes, or whether systematic regional differences exist. The amplitudes and phase constants of both S_1 and S_2 undergo large seasonal variation, very much larger at these high levels than at the earth's surface.

The oscillation also changes with elevation, the amplitude increasing, and the time of the maximum being delayed, with ascent from 80 to 100 kilometers. But the observations are not yet numerous enough to provide a basis for reliable quantitative determinations.

Unfortunately, very few data are available for the layers intermediate between the surface level and the meteor levels (80 to 100 km). Harris *et al.* (*7*) have published data on the diurnal and semidiurnal pressure and wind oscillations for Lajes Field at Terceira, Azores, based on balloon observations. These data are for levels lower than 30 kilometers. Up to this altitude no very pronounced vertical changes in S_1 and S_2 are found.

Like the solar tide the lunar tide must increase with elevation. But the data are not sufficient for determining it at meteor levels. One can only say that the winds due to the lunar tide must be less than 2 meters per second. At the surface the lunar tidal winds have a velocity about 100 times less than this value. Higher up, in the ionosphere, the lunar tidal oscillation can clearly be seen in various observable quantities, such as the geomagnetic parameters referred to earlier (*8*). The lunar oscillation has also been demonstrated to exist in other parameters, such as the virtual height of the E layer.

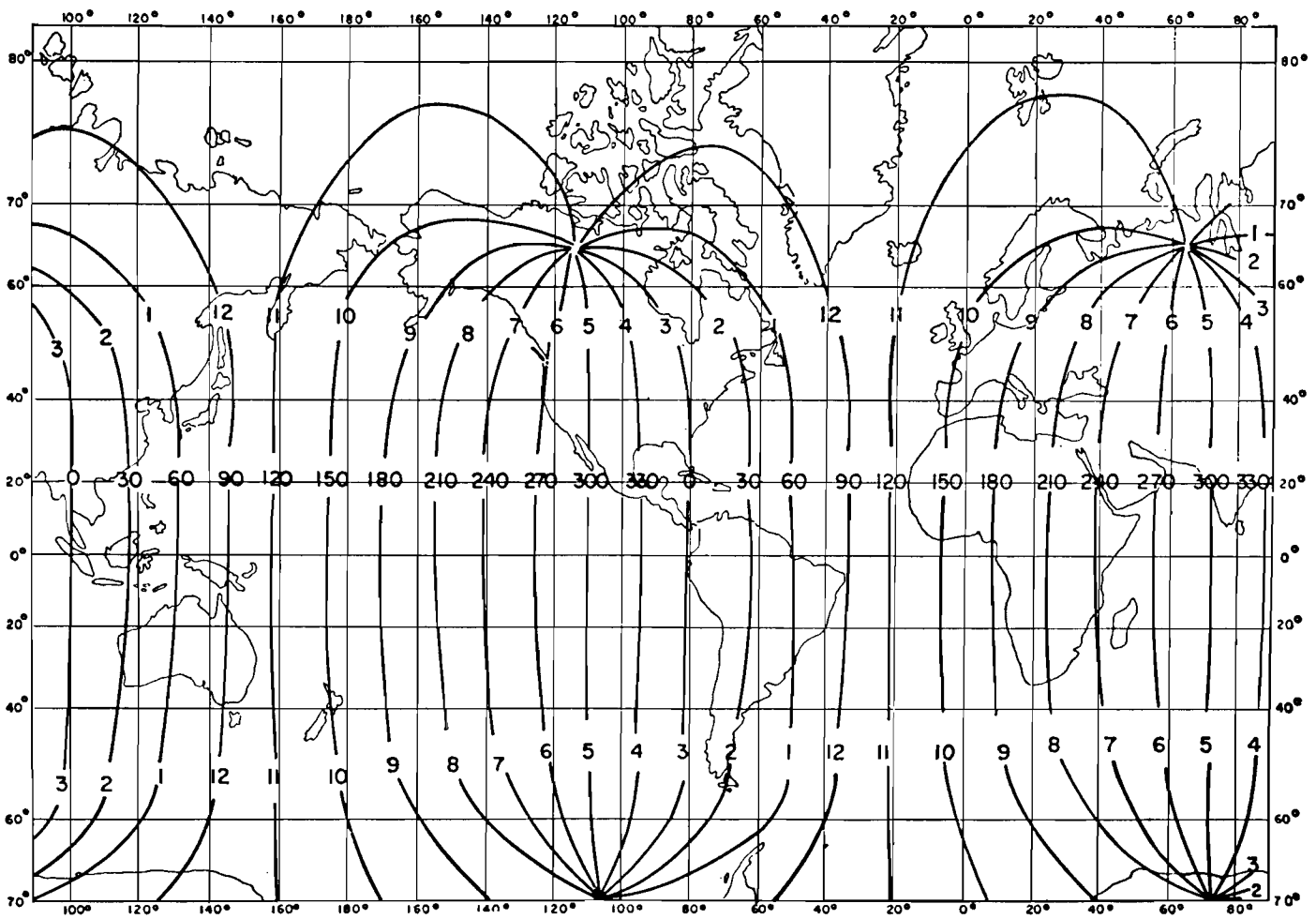

Fig. 5. Lines of equal phase for the semidiurnal solar tide as manifested in atmospheric pressure at the earth's surface (see *16*). The phase constants are given (near the center line of the map) in degrees, and (above and below the center line) in time (U.T.) of maximum pressure.

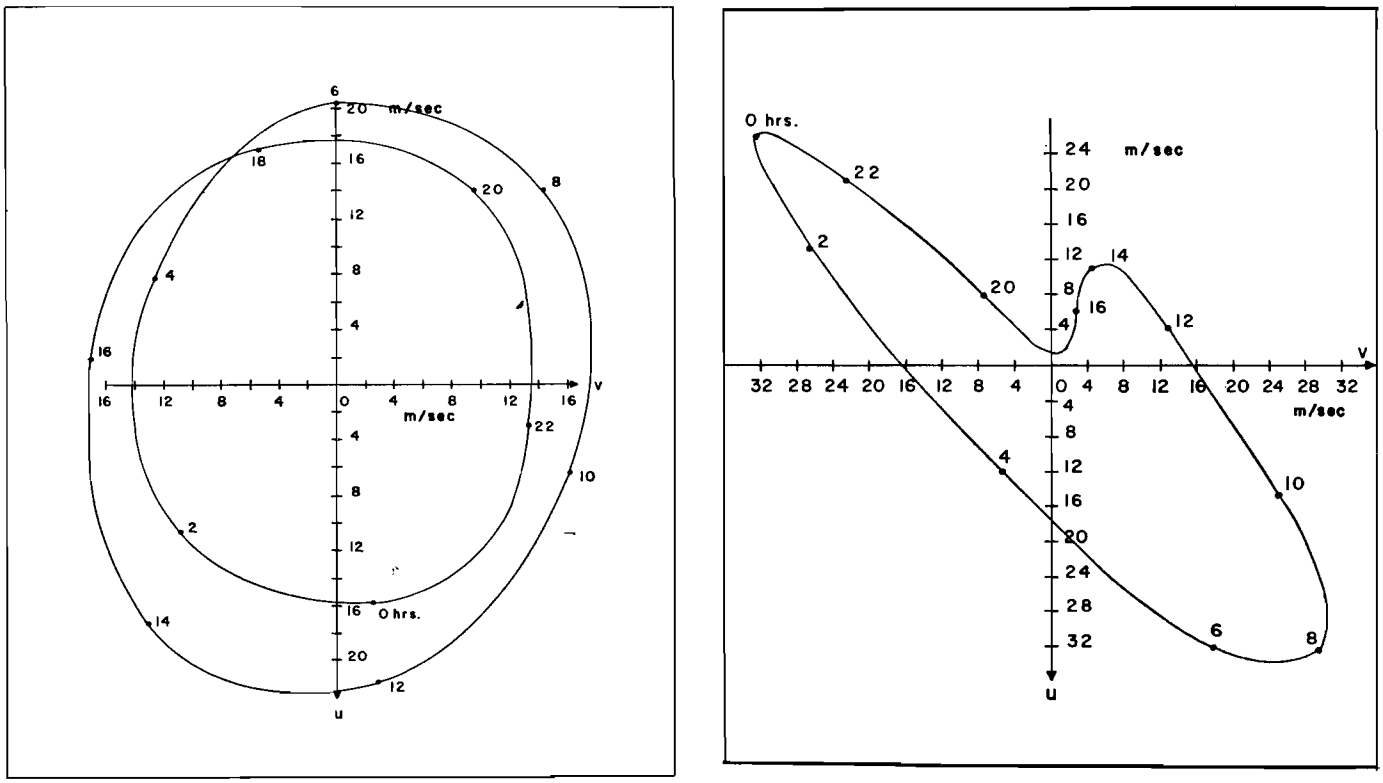

Fig. 6. Hodographs of the periodic components ($S_1 + S_2$) of the wind vector at altitudes of 80 to 100 kilometers during the *D* months (November through February), in meters per second, at (left) Jodrell Bank, England and (right) Adelaide, Australia. The curves represent the end points of the periodic wind vectors. The numbers adjoining the curves are hours, in local mean time.

Daily Temperature Variation

As I have explained, the solar tidal oscillations, including S_2, are probably due to the thermal rather than the gravitational action of the sun on the atmosphere. Therefore, let us consider at this point, as a manifestation of this thermal action of the sun, the daily temperature curve with its various harmonics, in order to understand how this daily temperature wave can produce a semidiurnal effect.

The solid curve of Fig. 7 shows, as a typical example, the daily variation in air temperature near the ground at Potsdam, Germany, during February; it is based on the average for data accumulated over 60 years. The temperature rises sharply from a minimum at about sunrise (about 7 a.m.) to a maximum at about 2 p.m. From there it decreases, first rapidly, then, especially after sunset (about 5 p.m.), much more gradually to its minimum. Thus, the diurnal temperature curve is not a simple sine curve with a 24-hour period but is asymmetrical. This asymmetry is due to the different processes determining the warming and cooling of the atmosphere. During the daytime the amount of radiative energy received depends largely on the altitude of the sun above the horizon, which follows, very approximately, a sine function; after sunset this energy flux is zero. The heat loss due to radiation is fairly constant throughout the day and night, so it is only throughout the daylight hours that the temperature curve can be expected to have a form approximating a sine curve. The sine curve with 24-hour period which gives the best fit (within the meaning of the method of least squares, the curve being obtained by harmonic analysis) is shown by the dashed curve (to which the daily mean has been added) of Fig. 7. To reproduce the more gradual temperature decrease at night, the delay of the minimum until the time of sunrise, and the more rapid rise and fall of the temper-

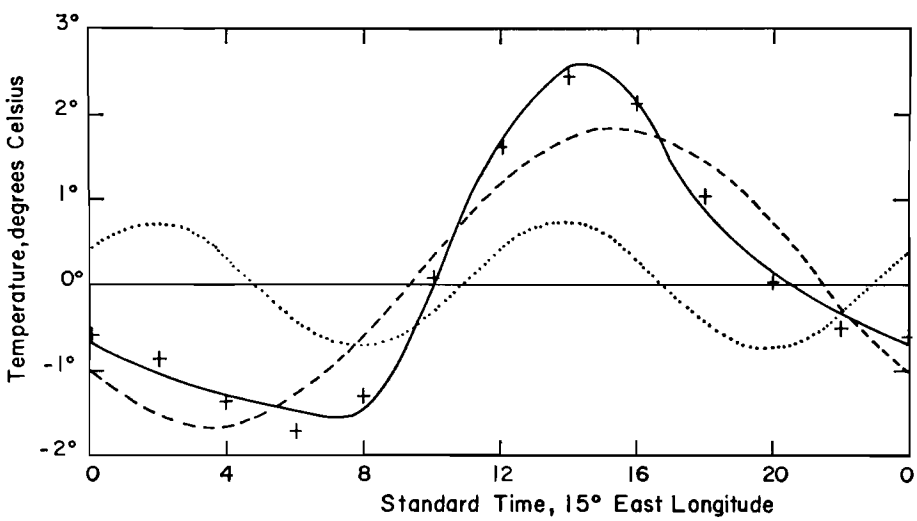

Fig. 7. (Solid curve) Daily variation of the air temperature at Potsdam, Germany, during February; (dashed curve) 24-hourly temperature wave; (dotted curve) 12-hourly temperature wave; (crosses) sum of these two waves.

ature during the daylight hours, one must add a sine curve with a period of 12 hours (the dotted line of Fig. 7). The superposition of the daily mean and the first and second harmonics is represented by the crosses for every second hour. The second harmonic of the daily temperature curve is thus a result of the asymmetry of the effects producing the temperature curve.

The remaining small difference between observed and computed temperatures can be largely represented by a third harmonic, a wave of 8-hour period; addition of this third harmonic corrects essentially for differences in the relative lengths of day and night throughout the year. It is zero or nearly zero around the equinoxes and changes its phase by 180 degrees (or nearly 180 degrees) between winter solstice and summer solstice, just like the corresponding pressure oscillation. A further improvement of the theoretical temperature curve can be obtained by adding a fourth harmonic, which has an amplitude even smaller than that of the third harmonic but which makes itself felt nevertheless as a corresponding small pressure oscillation of 6-hour period.

The breakdown of the daily temperature variation into a number of oscillations of different periods gives, of course, a purely formal result. The atmosphere, as an oscillating system, responds to the total excitation provided by the daily temperature oscillation. But the response depends on the tuning of the atmosphere to the different harmonics of the exciting force. Thus the amplitude ratios of, say, the pressure waves may be quite different from those of the temperature waves.

The Resonance Theory

Now let us return to the problem of the relative magnitudes of S_2 and L_2. Since L_2 is smaller than S_2, it is surmised that S_2 is probably largely attributable to the thermal, rather than to the gravitational, action of the sun. But the diurnal term in the daily-temperature curve is about 2.5 times the semidiurnal term (*9*), while the diurnal surface-presure oscillation is only about half the semidiurnal oscillation. To remove this difficulty Kelvin (*2*) advanced the resonance theory, according to which the atmosphere has a free oscillation with a period of about 12 hours. A great amount of theoretical

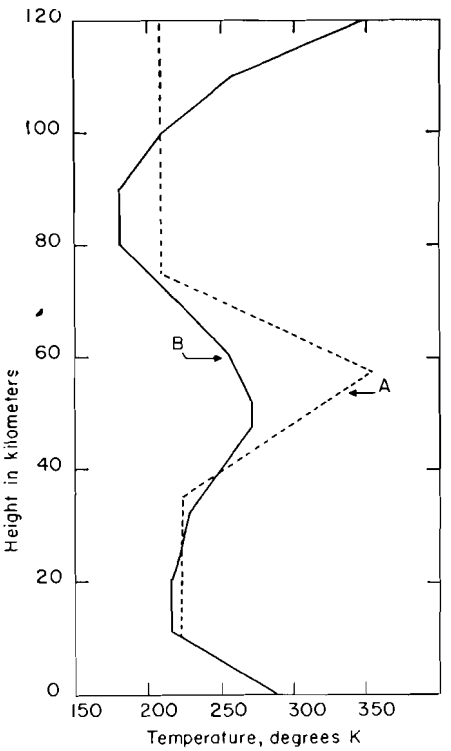

Fig. 8. Vertical temperature distribution in the atmosphere. (*A*) Temperature distribution assumed by Pekeris (*11*); (*B*) U.S. Standard Atmosphere curve, 1962 [U.S. Government Printing Office, Washington, D.C., 1962].

work has been done since Kelvin's time to determine the free oscillations of the terrestrial atmosphere and the response of the atmosphere to both gravitational and thermal types of excitation. From these investigations it follows that the free oscillations of the atmosphere are the same as the free oscillations of an incompressible and homogeneous ocean of "equivalent depth" h. This quantity h depends on the vertical temperature distribution of the atmosphere. G. I. Taylor (*10*) has shown that there is in general an infinite number of equivalent depths for a given atmospheric temperature distribution, and that h is related to the velocity V of long atmospheric waves by the formula $V^2 = gh$, where g is the acceleration of gravity. Such waves were observed during the eruption of the volcano Krakatao in 1883 and gave $h = 10$ km, approximately. On the other hand, according to theory the equivalent depth $h = 7.8$ km is required for a free oscillation with period of 12 solar hours.

In order to discuss what values the equivalent depth h of the real atmosphere may assume, let us consider Fig. 8, which represents two vertical atmospheric temperature distributions. Before rocket data became available, the information about the temperature distribution above 30 kilometers, then the ceiling of meteorological balloon ascents, came mainly from observations of the anomalous propagation of sound. These observations indicated, for altitudes around 50 kilometers, temperatures well above those found at the ground, and Pekeris (*11*) showed that with the temperature profile *A* of Fig. 8, which is characterized by a temperature maximum of 350°K at 60 kilometers, two values are obtained for h—namely, 10 kilometers, as suggested by the Krakatao waves, and 7.8 kilometers, very close to the value required for strong resonance magnification. Since that time, however, rocket ascents have given a much more reliable picture of the temperature distribution of the atmosphere; this distribution is represented by profile *B* of Fig. 8, which shows temperatures considerably lower than 350°K at altitudes of 50 to 60 kilometers. With these lower temperatures the value $h = 10$ km is retained, but not the value $h = 7.8$ km. Thus, the resonance magnification for the solar semidiurnal oscillation is not strong (not $\times$ 60 or more, as was previously thought) but quite weak (on the order of $\times$ 3 or $\times$ 4).

For these more realistic models with little magnification of S_2, the lunar semidiurnal oscillation would be magnified to about the same extent as the solar semidiurnal oscillation, in agreement with the observed magnitude of the lunar tide.

Thermal Excitation

With this low resonance magnification the gravitational excitation cannot contribute noticeably to the observed magnitude of the solar semidiurnal pressure oscillations. It becomes necessary to examine the thermal excitation in detail. Only a small amount of the incoming solar-radiation energy is absorbed in the atmosphere before reaching the ground. Thus, the heating of the atmosphere, at least in the lower troposphere, proceeds mainly from the ground upward, by turbulence and by long-wave radiation. These processes are effective only through a very limited height range. Hence, the resulting temperature oscillation is reduced to insignificance at a few hundred meters' altitude and affects only a small part of the total mass of the atmosphere,

one-tenth or less. So long as only this part of the total heating and cooling effect of the sun was considered, it seemed necessary to assume large magnification, and the contribution of the thermal excitation appeared to be only of about the same magnitude as the gravitational excitation (*12*), insufficient to explain the observed semidiurnal pressure oscillation without very appreciable magnification.

As a way out of this difficulty, Sen and White (*13*) and Siebert (*13*) pointed out that the amount of incoming solar energy absorbed directly in the atmosphere, while small, must give rise to a daily temperature variation in the atmosphere which makes a very significant contribution to the atmospheric oscillation, since it affects the whole atmosphere.

Moreover, at higher layers in the atmosphere, ozone becomes important in the atmospheric heat budget. Because of its high absorptive power in certain parts of the ultraviolet region the ozone that is present heats the upper atmosphere between 30 and 50 kilometers very considerably and is in fact responsible for the relatively high temperatures at about 50 kilometers shown in Fig. 8. The ozone also produces pronounced daily temperature variations in this whole layer, which must contribute to the diurnal oscillations and their higher harmonics. Butler and Small (*14*), in fact, conclude that by far the largest part of the semidiurnal pressure oscillation is due to the temperature oscillation in the ozone layer. If the temperature wave producing S_2 occurs mainly in a higher atmospheric layer, a node for S_2 should exist at about 30 kilometers, and the phase should here change by 180 degrees (*14, 15*). The geomagnetic variations seem to indicate a phase reversal between the surface layers of the atmosphere and the ionosphere. But this phase difference can also be accounted for by the gradual phase changes of S_2, observed in the tidal wind oscillations at meteor heights, between 80 and 100 kilometers. Data obtained in observations over the Azores (*7*) at elevations around 30 kilometers do not show the node and sudden phase change which should exist if the cause of S_2 is to be found in the ozone layer, but the elevations were not sufficiently high to rule it out conclusively. Thus, it is at present impossible to decide on observational grounds whether S_2 is caused by the heating of the whole atmosphere or by the heating of the ozone layer alone.

It remains for me to explain why the diurnal pressure oscillation at the ground is only half S_2, even though the corresponding diurnal temperature oscillation is about 2.5 times the semidiurnal temperature wave. The explanation of this discrepancy is to be found partly in the resonance magnification of S_2, even though this magnification is small, and partly in the fact that the diurnal pressure oscillation is actually reduced in the atmosphere, rather than magnified. This reduction is due to the small equivalent depth required for S_1—less than 700 meters, a value which differs from the actual equivalent depth of the atmosphere (10 km) even more than the value required for S_2 (7.8 km) does. A simple calculation based on Siebert's work shows that a temperature oscillation of a given amplitude would produce a 12-hourly pressure oscillation of amplitude almost 4 times that of the 24-hourly oscillation. Thus, the discrepancy between (i) the amplitudes of $S_2(p_0)$ and $S_1(p_0)$ and (ii) the amplitudes of the corresponding temperature oscillations is greatly reduced.

In the discussion of the tidal theory given here I refer only to the lower layers of the atmosphere, up to approximately 100 kilometers. At greater elevations, where the tidal motions become as large as the mean motion, the basic assumption of the tidal theory—that the motion is sufficiently small that the equations can be linearized—is no longer valid. Furthermore, because of the increasing ionization of the atmosphere at these heights, hydromagnetic effects can no longer be neglected. The study of these problems has hardly begun.

Summary

The semidiurnal lunar tide in the earth's atmosphere is about 15 times smaller than the semidiurnal solar tide. Since the gravitational tidal force of the moon is 2.2 times that of the sun, the semidiurnal solar tide must be largely produced by the thermal action of the sun. The daily variation of the atmospheric temperature has, in fact, not only a 24-hourly but also a 12-hourly harmonic and other, higher harmonics, because of the asymmetry of the daily temperature curve. The amplitude of the 24-hourly harmonic of the temperature curve is considerably larger than that of the 12-hourly harmonic. To explain why the 12-hourly pressure oscillation is larger than the 24-hourly oscillation, the resonance theory postulates that the atmosphere has a free oscillation of period close to 12 hours, so that the 12-hourly pressure oscillation is greatly magnified. But such a free oscillation requires, at elevations around 50 kilometers, temperatures higher than those at the ground, and rocket observations do not show such high temperatures. That the semidiurnal pressure oscillation is nevertheless larger than the diurnal oscillation can be accounted for by the fact that the atmosphere does magnify the 12-hourly oscillation slightly, and that it has a tendency to suppress the 24-hourly oscillation.

While the atmospheric tidal motions are small at the bottom of the atmosphere, as compared to the mean values for the wind velocity, they increase with altitude and are greater by about two orders of magnitude at elevations between 80 and 100 kilometers than they are at the earth's surface. Thus, strong periodic motions occur at these high levels.

References and Notes

1. The millibar (mb) is the pressure unit now generally used in meteorology. It is 1000 times the pressure unit (dyne/cm²) in the centimeter-gram-second system.
2. W. Thomson (later Lord Kelvin), *Proc. Roy. Soc. Edinburgh* **11**, 396 (1882).
3. See, for instance, S. Chapman and J. C. P. Miller, *Monthly Notices Roy. Astron. Soc., Geophys. Suppl.* **4**, 649 (1940).
4. See S. Chapman and K. C. Westfold, *J. Atmospheric Terrest. Phys.* **8**, 1 (1956), and earlier references given in that article.
5. B. Haurwitz, *Meteorol. Papers* **2**, No. 5 (1956).
6. J. S. Greenhow and E. L. Neufeld, *Quart. J. Roy. Meteorol. Soc.* **87**, 472 (1961); W. G. Elford, *Planetary Space Sci.* **1**, 94 (1959).
7. M. F. Harris, F. G. Finger, S. Teweles, *J. Atmospheric Sci.* **19**, 136 (1962).
8. S. Matsushita, in *Handbuch der Physik*, J. Bartels, Ed. (Springer, Berlin, 1964), vol. 49, p. 1.
9. B. Haurwitz, *Arch. Meteorol. Geophys. Bioklimatol.* **A12**, 426 (1962).
10. G. I. Taylor, *Proc. Roy. Soc. London* **A156**, 318 (1936).
11. C. L. Pekeris, *ibid.* **A158**, 650 (1937).
12. S. Chapman, *Quart. J. Roy. Meteorol. Soc.* **50**, 165 (1924).
13. H. K. Sen and M. L. White, *J. Geophys. Res.* **60**, 483 (1955); M. Siebert, thesis, Göttingen (1955); ———, *Advan. Geophys.* **7**, 105 (1961).
14. S. T. Butler and K. A. Small, *Proc. Roy. Soc. London* **A274**, 91 (1963).
15. R. Sawada, *J. Meteorol. Soc. Japan* **40**, 303 (1962); A. Matsushima and R. Sawada, *ibid.*, p. 309.
16. Figures 4 and 5 are based on a spherical harmonic analysis of the distribution of $S_2(p_0)$.